

Quark Medical Alignment: A Holistic Multi-Dimensional Alignment and Collaborative Optimization Paradigm

Tianxiang Xu^{*†1,2}, Jiayi Liu^{*‡1}, Yixuan Tong¹, Jialu Xu¹, Yunqing Wei¹, Kaiwen Feng¹, PanPan Hou¹, Kangping Yin¹, Jiyuan Hu^{†1,2}, Hao Zhou^{†1,2}, Zhenxin Ma¹, Jian Xu¹ and Guanjun Jiang¹

¹Qwen Applications Business Group, Alibaba, ²Peking University

^{*}These authors contributed equally to this work. [†]Work done during an internship at Alibaba. [‡]Corresponding author.

While reinforcement learning for large language model alignment has progressed rapidly in recent years, transferring these paradigms to high-stakes medical question answering reveals a fundamental paradigm mismatch. Reinforcement Learning from Human Feedback relies on preference annotations that are prohibitively expensive and often fail to reflect the absolute correctness of medical facts. Reinforcement Learning from Verifiable Rewards lacks effective automatic verifiers and struggles to handle complex clinical contexts. Meanwhile, medical alignment requires the simultaneous optimization of correctness, safety, and compliance, yet multi-objective heterogeneous reward signals are prone to scale mismatch and optimization conflicts. To address these challenges, we propose a robust medical alignment paradigm. We first construct a holistic multi-dimensional medical alignment matrix that decomposes alignment objectives into four categories: fundamental capabilities, expert knowledge, online feedback, and format specifications. Within each category, we establish a closed loop of where observable metrics inform attributable diagnosis, which in turn drives optimizable rewards, thereby providing fine-grained, high-resolution supervision signals for subsequent iterative optimization. To resolve gradient domination and optimization instability problem caused by heterogeneous signals, we further propose a unified optimization mechanism. This mechanism employs Reference-Frozen Normalization to align reward scales and implements a Tri-Factor Adaptive Dynamic Weighting strategy to achieve collaborative optimization that is weakness-oriented, risk-prioritized, and redundancy-reducing. Experimental results demonstrate the effectiveness of our proposed paradigm in real-world medical scenario evaluations, establishing a new paradigm for complex alignment in vertical domains.

1. Introduction

With the rapid advancement of RL for LLMs in recent years, researchers have increasingly recognized that relying solely on supervised fine-tuning (SFT), which heavily depends on large-scale high-quality annotated data, is insufficient to sustainably support performance improvements in complex instruction following, long-horizon reasoning, and interactive decision-making. In contrast, RL optimizes model behavior through a closed-loop process of generation–evaluation–update, enabling direct optimization toward target behaviors and providing a degree of self-improvement capability in out-of-distribution scenarios (Ouyang et al., 2022). Against this backdrop, two dominant technical paradigms have gradually emerged. The first is reinforcement learning from human feedback (RLHF), which aligns models with human intent and interaction preferences by leveraging human preference annotations or learned reward models (Bai et al., 2022). The second is reinforcement learning with verifiable rewards (RLVR), which employs automatically verifiable evaluators—such as mathematical answer checking, unit tests for code, or formal proof verification—to deliver more objective and scalable reward signals, thereby enhancing model reliability and reasoning ability on measurable tasks (Guo et al., 2025).

However, when transferring these advanced paradigms to the high-risk, long-tailed, and knowledge-intensive domain of medical question answering (Medical QA), we encounter a fundamental paradigm mismatch. On the one hand, preference annotation required by RLHF is prohibitively expensive and difficult to standardize in medical settings: annotators must possess professional medical qualifications, and a single clinical question often admits multiple reasonable formulations and diverse diagnostic or treatment pathways (Singhal et al., 2023), making it difficult to con-

sistently rank answers by quality. Moreover, human preferences tend to emphasize fluency and readability, which do not necessarily correspond to clinical correctness or safety. On the other hand, RLVR is also challenging to directly apply in medical scenarios. Most medical questions lack executable automatic verifiers; correctness is often conditional on patient history, examination results, and temporal progression, while medical knowledge continuously evolves and clinical guidelines vary across regions and institutions (Wu et al., 2025). More importantly, the objective of medical QA is not merely to produce a single “correct” answer, but rather to solve a multi-objective optimization problem under incomplete information. A medical model must simultaneously satisfy correctness, completeness, applicability, and safety: it must ensure strict factual accuracy, recognize uncertainty and missing information and proactively request clarification, adhere to complex clinical standard operating procedures (SOPs) for risk stratification and contraindication screening, produce compliant responses within the boundaries of non-diagnostic and non-prescriptive roles, and maintain empathetic communication with patients. These critical requirements are difficult to capture with a static, binary reward function. Meanwhile, multi-dimensional heterogeneous reward signals introduce scale mismatch and potential conflicts among optimization objectives, rendering traditional static linear weighting strategies ineffective and often leading to gradient domination or catastrophic forgetting during training (Lin et al., 2024).

To address these challenges, we propose a novel medical alignment framework, **MAP**. Our core insight is that robustness in medical agents must begin with a panoramic deconstruction of alignment objectives and culminate in adaptive collaboration among multi-source signals. Accordingly, we first construct a panoramic, multi-dimensional medical alignment paradigm that integrates an orthogonal and complementary heterogeneous evaluation matrix encompassing foundational capabilities (correctness and usefulness), expert knowledge, user feedback, and formatting compliance. Additionally, beyond building Bradley–Terry-based ORM preference reward models across multiple dimensions, we innovatively introduce a *Rubrics As a Reward* mechanism, which transforms abstract clinical pathways into executable and verifiable hard scoring criteria, thereby providing stable “expert-style constraints” (Gunjal et al., 2025). To obtain finer-grained and interpretable supervision, we further combine a generative assertion reward model—which decomposes responses into verifiable assertions with evidence-driven feedback—with PRM process supervision, which characterizes risk-prone segments based on generation-time confidence. Together, these components form a unified error decomposition perspective that delivers higher-resolution training signals for subsequent policy optimization and iterative refinement (Lightman et al., 2023; Zhang et al., 2024).

Building upon this foundation, to mitigate the dynamical instability induced by multi-dimensional heterogeneous reward signals during reinforcement learning, we propose the **Uni-Reward** collaborative optimization mechanism. Uni-Reward abandons conventional static linear weighting schemes and instead adopts an adaptive strategy that combines distribution normalization based on stationary statistics with tri-factor dynamic weighting. By continuously sensing task difficulty, safety confidence, and signal redundancy, Uni-Reward dynamically adjusts the optimization trajectory, effectively resolving gradient masking caused by scale mismatch. This ensures that improvements in response friendliness and formatting compliance are achieved without sacrificing core medical accuracy or safety, enabling the model to identify an optimal trade-off under multiple constraints on a complex Pareto surface.

The main contributions of this work are summarized as follows:

- **Holistic Medical Alignment Paradigm.** We propose a holistic multi-dimensional medical alignment paradigm to address the coexistence of incomplete information and high-risk constraints in medical scenarios. Specifically, we construct an orthogonal and complementary evaluation matrix spanning four dimensions: foundational capabilities, expert knowledge, user feedback, and formatting compliance. By integrating outcome-based reward modeling (ORM), process reward modeling (PRM), generative reward modeling (GRM), and generative assertion-based reward modeling (GARM), and further transforming clinical guidelines into verifiable rubric-based rewards, our framework provides a novel modeling perspective for tackling complex alignment challenges in vertical domains.
- **Uni-Reward Collaborative Optimization for Heterogeneous Signals.** To address the scale mismatch and gradient domination issues arising from the coexistence of multi-dimensional heterogeneous discrete rule constraints and continuous preference signals during reinforcement learning, we propose a general adaptive optimization framework termed **Uni-Reward**. This mechanism combines distribution normalization based on stationary statistics with a tri-factor dynamic weighting strategy that accounts for task difficulty, sample pessimism, and signal redundancy. As a result, Uni-Reward enables robust coordination of heterogeneous gradients on non-convex optimization landscapes.
- **Pareto-Optimal Trade-offs in Multi-Objective Medical Alignment.** Beyond demonstrating overall performance improvements, we conduct extensive ablation studies and training dynamics analyses to reveal Pareto-optimal trade-offs in multi-objective medical alignment. Our results confirm the effectiveness of Uni-Reward in mitigating the *alignment tax*. Empirically, the proposed approach effectively avoids catastrophic forgetting when pursuing high factual accuracy, while maximizing response usefulness and empathy under strict medical safety constraints. These

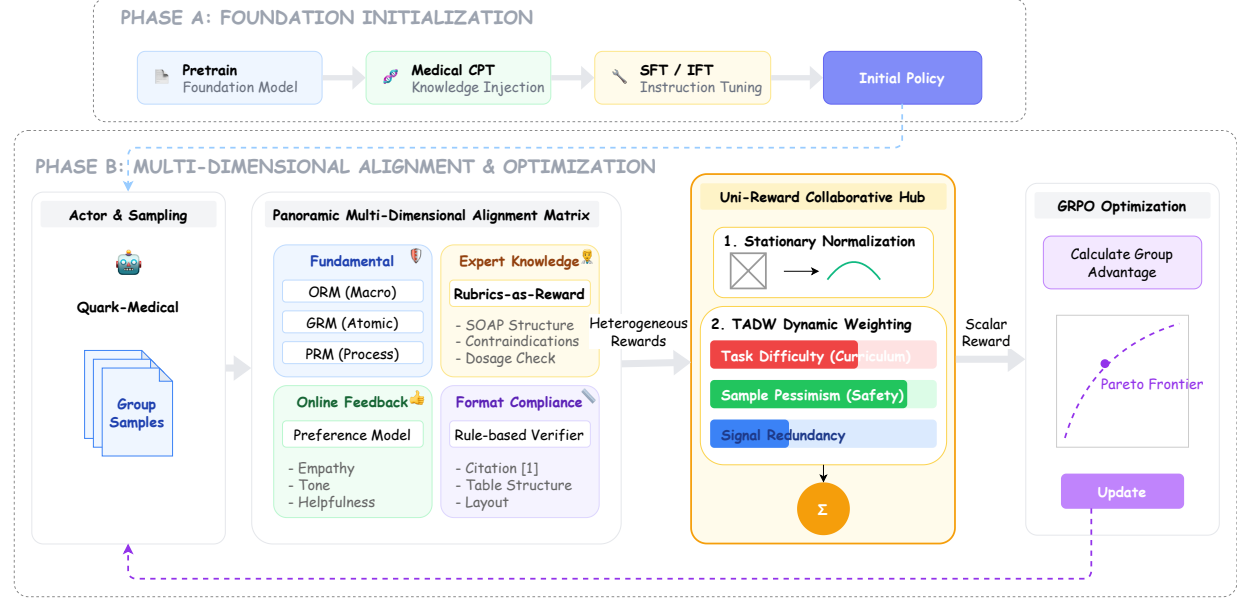


Figure 1 | The proposed Medical Alignment Paradigm (MAP) which involves a holistic multi-dimensional medical alignment matrix and a uni-reward optimization mechanism for reinforcement learning.

findings provide both empirical evidence and theoretical insights for alignment research in high-risk domains.

2. Overview

To achieve robust alignment of large language models in medical scenarios characterized by incomplete information and high-risk constraints, we design this medical alignment paradigm as a data-driven, multi-stage evolving closed-loop feedback control system. As illustrated in Fig. 1, the framework follows a *Deconstruction–Collaboration* control-theoretic paradigm, integrating an end-to-end pipeline ranging from foundation enhancement and expert behavior cloning to reinforcement learning optimization.

Medical Knowledge Injected Foundation Initialization. The system cold-start is built upon the powerful QuarkMed Medical Foundation Model (Li et al., 2025a). To ensure that the initial policy exhibits rigorous clinical reasoning and robust instruction-following capabilities, we adopt a construction strategy that prioritizes high-quality real-world data supplemented by synthetic data. Specifically, we first perform domain-adaptive continual pretraining (CPT) on medical corpora, enabling the model to absorb multi-source knowledge including clinical guidelines and consensus documents, textbooks and medical literature, drug labels, and de-identified electronic medical records. Subsequently, we conduct refined instruction fine-tuning (IFT/SFT) on high-quality instruction datasets, where complex reasoning and safety-critical scenarios are selectively augmented through Self-Instruct and Red-Teaming. This process is further enhanced by retrieval-augmented generation (RAG) and Best-of- N selection mechanisms to improve alignment quality. Through this two-stage “pretraining–instruction alignment” injection process, implicit medical knowledge and clinical norms are explicitly consolidated into model parameters, yielding an initial policy π_{sft} endowed with foundational medical competence and usable conversational behavior.

Panoramic Multi-Dimensional Medical Alignment Matrix. During the reinforcement learning stage, to precisely capture subtle deficiencies in model generations, we orthogonally decompose complex medical alignment objectives into four independent and measurable matrix spaces: foundational capability alignment, expert knowledge alignment, online feedback alignment, and formatting compliance alignment. Each matrix space is further designed as a closed loop of “observable metrics–attributable diagnosis–optimizable rewards”. On the foundational capability side, correctness and usefulness serve as core objectives. Correctness is assessed via a multi-granularity orthogonal verification mechanism (macro-level ORM, atomic-level GARM, and micro-level PRM-CRD), while usefulness is evaluated through a six-dimensional framework (HDUF), together producing stable preference signals. On the expert knowledge side, Auto-Rubrics explicitly operationalize clinical guidelines into executable scoring rules, with non-linear scoring and distillation employed to enhance robustness and efficiency. On the online feedback side, generative reward modeling (GRM) is used to denoise and attribute sparse, high-noise thumbs-up/thumbs-down signals, converting them

into high-quality pairwise preference samples. On the formatting side, verifiable constraints and reward terms are constructed around highlighting, tabular structures, and authoritative citations. Collectively, these components yield a unified and interpretable error decomposition, providing fine-grained, high-resolution supervision signals for subsequent iterative optimization.

Uni-Reward Collaborative Optimization. To resolve structural disparities among heterogeneous rewards in terms of scale, sparsity, and learnability, we introduce Uni-Reward as a unified optimization layer. The design of this layer also follows a closed-loop paradigm of “observable statistics–attributable instability–optimizable weights”. Specifically, all reward components are first projected into a unified and stable scale coordinate system via Reference-Frozen Normalization. Subsequently, a Tri-Factor Adaptive Dynamic Weighting (TADW) mechanism is applied, where a bottleneck-oriented difficulty/curriculum factor, a risk-prioritized pessimism factor, and an information-gain-driven de-redundancy factor jointly modulate the weights. This enables semantically aware and stable collaborative optimization, resulting in smoother training curves, improved convergence, and more reliable gains in clinical competence. Finally, the composite scalar reward produced by Uni-Reward is used to guide the Group Relative Policy Optimization (GRPO) algorithm, driving the policy network π_θ to robustly evolve toward the Pareto frontier that complies with medical ethics and clinical standards on a non-convex optimization surface (Shao et al., 2024).

3. Multi-Dimensional Alignment Rewards

3.1. Foundational Capability Alignment: Multi-Granularity Orthogonal Verification for Correctness

As LLMs are increasingly deployed in high-risk domains such as clinical decision support and medical consultation, hallucinations and factual errors have become a primary bottleneck preventing their trustworthy real-world adoption. Unlike open-domain conversational settings, incorrect information in medical scenarios can directly lead to severe patient safety risks, placing exceptionally stringent requirements on correctness from both AI governance standards and user trust mechanisms. We therefore treat correctness optimization as a systematic engineering problem rather than a single-metric improvement task. Constructing a robust Correctness Detector forms the cornerstone of this effort: it serves not only as a critical reward signal during reinforcement learning alignment, but also supports data filtering during SFT and post-generation verification in RAG pipelines.

To address the intrinsic complexity of medical fact verification, we move beyond single-view evaluation and propose a *Multi-Granularity Orthogonal Verification* mechanism, which expands correctness detection from a black-box scalar score into three complementary and cooperative pathways: macro, atomic, and micro. At the macro level, an augmented Bradley–Terry ORM performs holistic preference discrimination, where “tie” samples are explicitly incorporated to enhance boundary robustness. At the atomic level, a retrieval-augmented fact-checking agent decomposes responses into atomic assertions, retrieves authoritative evidence, and applies a dual-adjudicator mechanism to determine consistency and generate interpretable rewards, which is also called generative assertion reward modeling (GARM). At the micro level, a PRM operates on token-level confidence signals, introducing *Contextual Relative Drop* (CRD) and robust aggregation methods (e.g., Bot- k) to localize high-risk segments. Together, these three components form a comprehensive and layered correctness verification system.

3.1.1. ORM: Macro-Discrimination via Augmented Bradley–Terry

As the first line of defense for correctness verification, the ORM aims to capture human preference distributions over the overall factual correctness of model responses. Following the classical RLHF paradigm, we formulate correctness discrimination as a pairwise ranking problem. Given an input x and two candidate responses y_{win} and y_{lose} , where y_{win} is factually more accurate than y_{lose} , the standard Bradley–Terry model optimizes a scalar reward function r_θ by minimizing the negative log-likelihood loss:

$$\mathcal{L}_{diff}(r_\theta) = -\mathbb{E}_{(x, y_{win}, y_{lose}) \sim \mathcal{D}_{diff}} [\log \sigma(r_\theta(x, y_{win}) - r_\theta(x, y_{lose}))].$$

However, real-world medical annotation faces severe challenges of data sparsity and sample ambiguity. Constructing high-quality medical correctness preference data requires costly expert resources, and annotation analysis reveals that up to 50% of sample pairs are judged by experts as exhibiting *no significant correctness difference* (ties). Conventional BT training paradigms typically discard such tied pairs, leading to substantial data waste and weakened discriminative capability near decision boundaries.

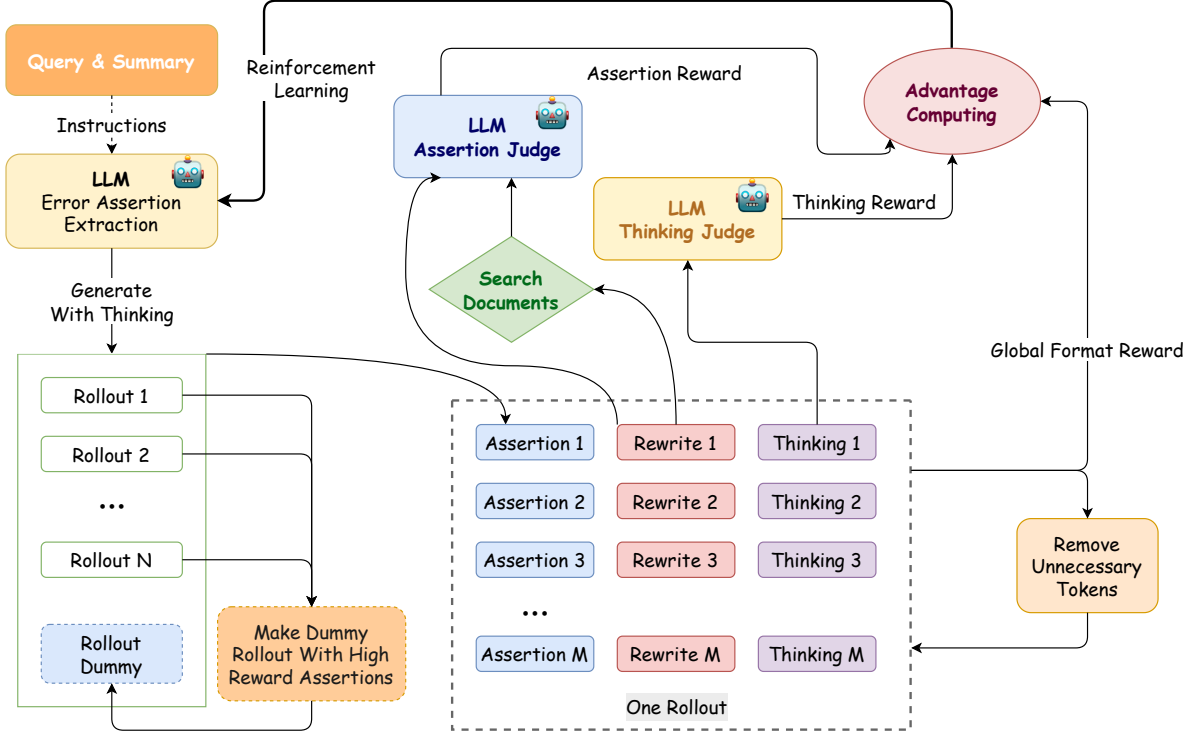


Figure 2 | Workflow of the Fact-checking Agent featuring retrieval-augmented dual-judge verification.

To address this limitation, we propose a *Margin-Constrained Preference Loss* that extracts supervision signals from tie samples. For pairs labeled as unordered (y_{same1}, y_{same2}) , we introduce an auxiliary loss term \mathcal{L}_{same} that regularizes the reward difference between the two responses:

$$\mathcal{L}_{same}(r_\theta) = -\mathbb{E}_{(x, y_{same1}, y_{same2}) \sim \mathcal{D}_{same}} [\log \sigma (\text{abs}(r_\theta(x, y_{same1}) - r_\theta(x, y_{same2})))].$$

The final optimization objective is given by $\mathcal{J} = \mathcal{L}_{diff} + \lambda \mathcal{L}_{same}$. Empirical results show that this hybrid optimization strategy effectively leverages boundary samples previously treated as noise, improving accuracy on medical correctness discrimination by 1%–2% and substantially enhancing robustness near ambiguous boundaries.

To further push the performance ceiling of the reward model, we construct a comprehensive optimization toolkit spanning data synthesis to model fine-tuning. For data augmentation, we employ stronger LLMs (e.g., Gemini3-Pro) to automatically identify logical flaws and generate synthetic preference pairs, while incorporating preference strength modeling to distinguish “clearly better” from “slightly better” responses, enhancing sensitivity to error severity. On the training side, we adopt multi-stage curriculum learning: large-scale synthetic data are first used for coarse alignment, followed by expert-annotated data for fine-tuning, maximizing sample efficiency. To mitigate catastrophic forgetting in multi-objective training, we apply domain-adaptive continued pre-training to reinforce medical representations and employ LoRA for parameter-efficient fine-tuning. Finally, to address long-tail medical knowledge verification, we explore retrieval-augmented reward modeling by providing authoritative external knowledge (e.g., clinical guidelines) as context, enabling the reward model to ground its preferences in factual evidence.

3.1.2. GARM: Atomic Fact-Checking via Retrieval Augmentation

Although LLMs exhibit strong performance in general knowledge domains, relying solely on internal parametric knowledge for factual judgment in long-tail, high-risk medical scenarios often leads to hallucinations and outdated information. To construct high-confidence and interpretable correctness rewards, we design a retrieval-augmented *Fact-checking Agent*. Instead of end-to-end black-box scoring of long responses, the agent adopts a layered “atomization–retrieval–adjudication” paradigm. As shown in Fig. 2, the agent first decomposes complex medical responses into independent atomic assertions, retrieves authoritative external evidence, and applies reinforcement learning to optimize both extraction and adjudication.

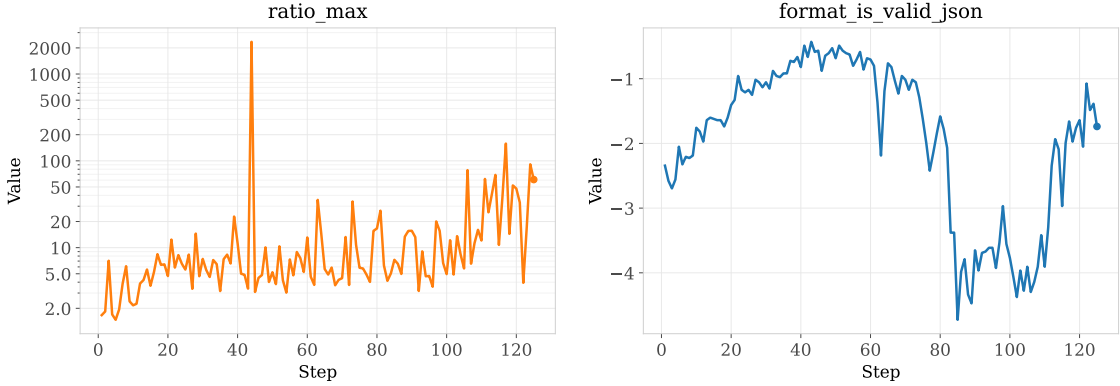


Figure 3 | Training instability in standard GRPO, characterized by extreme importance sampling ratio spikes and subsequent performance degradation.

Atomic Assertion Extraction under Structural Constraints The primary challenge in fact verification lies in extracting verifiable minimal semantic units from unstructured long-form text. We define an *atomic assertion* as a self-contained declarative statement expressing a single medical fact. To ensure completeness and formatting consistency, we fine-tune a dedicated extractor and impose vLLM Structured Outputs decoding constraints to enforce strict JSON Schema compliance. Nevertheless, even after supervised fine-tuning, the extractor may suffer from hallucinated content or over-extraction. To address this, we introduce outcome-supervised reinforcement learning to further optimize the extraction policy. As summarized in Table 1, we design a composite reward function R_{extract} that positively rewards high-quality assertions overlapping with human annotations while penalizing invalid, redundant, or malformed outputs, achieving an optimal balance between recall and precision.

Table 1 | Design of the composite reward function for the Assertion Extractor.

Reward Component	Type	Description	Aggregation
FORMAT_IS_VALID_JSON	Global	Validates whether the output follows a syntactically correct JSON format.	Weighted Sum
RESULT_COUNT_UP_BOUND	Global	Penalizes the extraction of excessive assertions.	Weighted Sum
FORMAT_FIELD_NAME_CHECK	Local	Verifies whether the current dictionary object contains required keys.	Length-normalized Weighted Sum
FORMAT_FIELD_VALUE_CHECK	Local	Ensures that the values within the dictionary object conform to expectations.	Length-normalized Weighted Sum
RESULT_GOLDEN_OVERLAP	Local	Measures the semantic overlap between the extracted assertion and the ground truth.	Top-N Element-wise Weighted Sum
RESULT_SUMMARY_OVERLAP	Local	Evaluates the grounding of the assertion in the source text.	Top-N Element-wise Weighted Sum

Training Stability Optimization: GSPO and ListMLE As illustrated in Fig. 3, when training the extractor with GRPO, we observe significant instability caused by token-level importance sampling ratios that spike at specific tokens, leading to local gradient explosions. To resolve this, we introduce *Group Sequence Policy Optimization* (GSPO), which replaces token-level ratios with sample-level averaged ratios, effectively smoothing policy updates (Zheng et al., 2025). In addition, to address advantage estimation bias arising from high intra-group similarity and large inter-group variance among rollouts, we introduce the ListMLE loss. Unlike absolute score regression, ListMLE maximizes the likelihood of reward-induced rankings, focusing on relative ordering rather than absolute values. This formulation effectively suppresses inter-group noise and substantially improves discrimination under fine-grained differences.

Evidence Retrieval and Dual-Adjudication Mechanism Extracted atomic assertions are passed to a retrieval module that recalls Top- K relevant documents from authoritative medical databases. We then apply a dual adjudication mechanism. The *Assertion Judge*, implemented as a generative discriminator, evaluates consistency between assertions and retrieved evidence. To enhance robustness, we employ Chain-of-Thought reasoning and majority voting

across multiple rollouts. Complementarily, the *Thinking Judge* evaluates the reasoning trace for assertions involving complex clinical logic, assessing whether the generation process follows valid medical reasoning (e.g., consultation before prescription). Assertions validated by the Thinking Judge receive dynamically increased weights, encouraging models to reason correctly rather than merely output correct conclusions. Through leading this closed-loop system, the Fact-checking Agent transforms ambiguous long-form generation quality into interpretable, verifiable atomic-level correctness scores, compensating for limitations in parametric medical knowledge.

Experimental Evaluation and Performance Analysis To quantitatively evaluate the effectiveness of the Fact-checking Agent, we conduct extensive experiments on validation sets covering random samples, drug-specific domains, and SGS hard cases. As shown in Table 2, while introducing the adjudicator slightly degrades performance on non-factual general instructions, accuracy on the clinically critical R1-Drug metric improves by 7.5%. This demonstrates that retrieval-augmented adjudication effectively mitigates hallucinations on professional medical entities.

Table 2 | Performance Comparison of Assertion Extraction and Verification Systems.

Method	Macro-Avg	R1-Random	R1-Drug	SGS Macro-Avg
Assertion-GRM	60.32%	50.94%	53.75%	62.83%
Assertion-GRM + Judge	56.10%	51.35%	61.25%	56.97%

Further analysis of the core Assertion Judge is presented in Table 3. The results reveal a pronounced performance asymmetry: the model achieves high reliability in identifying correct samples (F_1 of 89.78%) but exhibits lower recall for incorrect samples, reflecting a conservative bias that leaves some subtle hallucinations undetected. Nevertheless, the high precision of 88.07% on positive samples ensures high-confidence reward signals, preventing erroneous penalties from degrading language generation during reinforcement learning. To address this recall bottleneck, we introduce a *sample pessimism factor* in subsequent Uni-Reward optimization.

Table 3 | Classification performance breakdown of the Assertion Judge.

Configuration	Class: Incorrect (Negative)	Class: Correct (Positive)
Qwen3-4B	$P = 55.88\%$	$P = 88.07\%$
ra=top10	$R = 34.55\%$	$R = 91.56\%$
3.5K Samples	$F_1 = 42.70\%$	$F_1 = 89.78\%$

3.1.3. PRM: Internal Probing via Context-Relative Drop

Although ORM and GRM perform well in macro-level discrimination and external factual verification, they are inherently lagging outcome-oriented evaluations. As such, they struggle to capture the micro-level uncertainty dynamics that arise during the generation process itself. Conventional scalar reward signals can reflect relative sample-level quality, but they fail to localize concrete error regions—such as factual inaccuracies, logical discontinuities, or misuse of rare medical terminology—which severely limits both interpretability and fine-grained optimization.

To address this limitation, we introduce an internal probing mechanism based on token-level log-probabilities. Prior work has shown that large language models intrinsically encode generalized reward assessment capabilities (Li et al., 2025e), and that there exists a deep mathematical connection between log-probability distributions and reward functions (Rafailov et al., 2024). Our objective is to open this black box and quantify uncertainty directly at the level of the generation mechanism, thereby constructing high-resolution process supervision signals.

Limitations of Absolute Thresholds and the Semantic Consistency Hypothesis Existing uncertainty quantification approaches predominantly rely on absolute thresholding, where tokens whose log-probabilities fall below a fixed cutoff (e.g., -10.0) are classified as hallucinations. However, in knowledge-intensive medical scenarios, such static strategies exhibit severe robustness limitations. Empirical observations indicate that low confidence does not necessarily imply incorrectness: it may arise from high-entropy functional words or from the inherent rarity of long-tail medical entities. Absolute thresholding fails to distinguish between “fluent errors” and “correct but rare terminology”, leading to systematic false positives that erroneously penalize high-value professional expressions and significantly degrade recall in complex medical settings. This challenge is widely recognized in hallucination detection, where reliance on single-token probabilities is often insufficient to identify nuanced semantic deviations (Farquhar et al., 2024).

To overcome this issue, we propose an adaptive validation method termed *Context-Relative Drop* (CRD), grounded in the *Semantic Consistency Hypothesis*. The hypothesis posits that within a logically coherent and factually correct sentence, the confidence of key entities should remain relatively stable with respect to the surrounding context, rather than exhibiting abrupt discontinuities. Following the “weakest-link” principle, the reliability of an entity is often determined by its most fragile component. Accordingly, for a target entity E , we define its relative drop $\mathcal{D}(E)$ as the difference between the minimum token log-probability within the entity span and the average log-probability of the entire sentence:

$$\mathcal{D}(E) = \min_{t \in E} (\log P(t)) - \frac{1}{|S|} \sum_{j=1}^{|S|} \log P(t_j),$$

where S denotes the complete sentence baseline containing the entity.

By introducing a sentence-level baseline, absolute confidence values are transformed into relative logical gaps, effectively decoupling contextual difficulty from error signals. This mechanism demonstrates superior diagnostic value in two extreme scenarios. In high-fluency hallucination cases, models often assign very high confidence to common connective phrases or generic sentence templates, while exhibiting sharp confidence drops when inserting key false facts. For example, when generating “Sodium guaiacol sulfate (entity) is a surfactant (high-frequency context)”, the sentence-level baseline may be high (e.g., -1.13), but the extremely low entity score (e.g., -19.41) results in a large relative drop (-18.28), thereby triggering a high-risk alert. Conversely, in long-tail professional terminology scenarios (e.g., “This suggests that the patient’s ulcerative colitis is in the active phase”), data sparsity may cause the model to assign uniformly low probabilities to the entire sentence (baseline -1.70 , entity -3.40). In this case, despite the low absolute entity score, the small relative drop (-1.70) indicates that the term is rare yet consistent with the overall contextual difficulty, and is therefore correctly exempted. Fundamentally, CRD constitutes a quantitative validation of textual semantic consistency, sensitively capturing “logical cliffs” where entity confidence collapses relative to a high-confidence context, thereby enabling robust self-consistency checking without reliance on external knowledge bases.

Multi-Strategy Aggregation for Interpretability. To transform token-level microscopic signals into sample-level macroscopic rewards, we construct a multi-strategy aggregation framework, with explicit treatments for length bias and positional bias. First, regarding the choice of base signal, our experiments consistently show that using the *Diff* signal—defined as the difference between the log-probabilities of the policy model and the SFT reference model—significantly outperforms raw LogProb. By subtracting the background probabilities of the SFT model, high-confidence noise induced by high-frequency tokens is effectively suppressed, such that the remaining signal more faithfully reflects the model’s true mastery of the specific context.

For aggregation operators, the conventional *Sum* strategy suffers from severe length dependency, leading to systematic misjudgment, while the *Mean* strategy, although alleviating length effects, fails to overcome the intrinsically high-entropy bias of sentence-initial tokens. In contrast, the proposed *Bot-k* strategy—defined as the mean of the lowest k token-level LogProb values—exhibits the best robustness. This strategy strikes a balance between sensitivity to extreme errors and overall evaluation stability, effectively mitigating the tendency of long texts to accumulate lower scores simply due to having more tokens. Empirically, accuracy as a function of k follows an inverted U-shaped or saturating growth trend. When the window size is expanded to $k = 20$, the strategy effectively acts as a “soft low-pass filter,” preserving critical error signals while smoothing sporadic prediction fluctuations. Although we also explored more sophisticated debiasing approaches, such as masking sentence-initial tokens (*mask_first_token*) and statistical normalization (*z_score*), *Bot-20* ultimately prevails in our experiments due to its simplicity and generalization capability, and is therefore adopted as the default choice in subsequent Uni-Reward optimization.

Experimental Validation. We conduct extensive evaluations of the above strategies under the DPO training framework. Table 4 indicate that, although token-level fine-grained methods achieve slightly lower absolute accuracy than the black-box BT-RM, the proposed composite approach yields a qualitative shift in the evaluation paradigm. Specifically, *Bot-20* is used for robust global quality ranking, while Context-Relative Drop enables interpretable entity-level hallucination diagnosis. Notably, the strategy combining the *Diff* signal with *Mean_z_score* demonstrates the strongest robustness under varying sequence lengths and achieves the most balanced length ratio (0.6328), underscoring the importance of mitigating positional bias in constructing fair reward signals. This dual-track mechanism of “macroscopic ranking plus microscopic diagnosis” not only improves the fairness of reward modeling for variable-length texts, but also provides transparent and attributable fine-grained evidence for subsequent high-quality data curation and human auditing.

Table 4 | Comparative analysis of reward model performance under different aggregation strategies. **Bot-20** and **z_score** demonstrate superior robustness and fairness across different baselines.

Method	length ratio	sum	mean	min	bot-5	bot-10	bot-20	mask first	z score
DPO-COR-RA	0.6169	0.6325	0.5695	0.5448	0.5852	0.6189	0.6329	0.5787	0.5718
DPO-COR-RA-DIFF	0.6169	0.6113	0.6291	0.5258	0.5372	0.5639	0.6083	0.6230	0.6328
DPO-COR	0.6169	0.6273	0.5658	0.5451	0.5921	0.6037	0.6040	0.5672	0.5670
DPO-COR-DIFF	0.6169	0.6153	0.5802	0.5627	0.5722	0.5746	0.5684	0.5994	0.5916
DPO-Qwen3	0.5973	0.6200	0.5287	0.5195	0.5782	0.5868	0.5947	0.5163	–
DPO-Qwen3-DIFF	0.5973	0.6269	0.5105	0.5056	0.6164	0.6267	0.6364	0.5113	–
DPO-Qwen3-RA	0.5973	0.6230	0.5561	0.5041	0.5860	0.6032	0.6150	0.5435	–
DPO-Qwen3-DIFF-RA	0.5973	0.6171	0.5169	0.5150	0.6215	0.6296	0.6622	0.5175	–

3.2. Foundational Capability Alignment: A Hexa-Dimensional Utility Evaluation Framework for Helpfulness

In the complex interactive setting of Medical QA, *helpfulness* is not a monolithic indicator of instruction following, but rather a composite capability jointly determined by relevance, logical soundness, completeness, harmlessness, practical applicability, and formatting experience. To transform this inherently subjective assessment into an optimizable and measurable supervision signal, we propose the Hexa-Dimensional Utility Framework (HDUF). Within the data flywheel, we adopt a three-level multi-granularity diagnostic annotation scheme at the discourse, paragraph, and sentence levels, accompanied by fine-grained positive/negative incentive labels and preference strength annotations. This design enables the RM to receive dense, attributable training signals.

Furthermore, to address key challenges in medical preference learning—namely length bias, the high proportion of Same/Tie samples, and gradient instability during early training—we introduce a set of robust training strategies, including length-aware sample balancing, a margin-constrained loss leveraging Same samples, and dynamic distribution clamping. Combined with continuous long-tail sampling and iterative policy updates, this closed-loop mechanism substantially strengthens the RM’s decision boundaries and generalization ability in complex medical contexts, with particularly notable gains in medium-difficulty samples and multi-turn interaction scenarios.

3.2.1. HDUF and Multi-Granularity Diagnosis

Conventional scalar reward models often struggle to disentangle specific deficiencies in model-generated responses. To this end, we decompose helpfulness in the medical domain into six orthogonal and complementary sub-dimensions, as summarized in Table 5. *Relevance* ensures alignment with user intent; *Logical Coherence* evaluates the self-consistency of medical reasoning chains; *Completeness* measures coverage of core clinical points; *Harmlessness* enforces ethical and safety boundaries; *Practicality* emphasizes actionable guidance; and *Format & Readability* focuses on structured and professional information presentation. This multi-dimensional framework not only provides dense gradient signals for RM training, but also establishes a de facto “gold standard” for medical LLM outputs.

In the annotation stage of the data flywheel, we abandon coarse overall scoring in favor of a “Multi-Granularity Diagnosis” strategy. Annotators conduct microscopic inspections of responses at the discourse, paragraph, and sentence levels (see Appendix A.3). To precisely capture pathological generation patterns, we construct a taxonomy of dozens of fine-grained *Negative Incentive Labels* (see Table 19). For example, within the logical coherence dimension, we distinguish between “core claim contradiction” and “localized logical confusion”; within relevance, we differentiate “severe intent deviation” from “weak instruction adherence”. Conversely, we design *Positive Incentive Labels* (e.g., “demonstrates medical humanistic care” or “well-supported by evidence”, see Table 20) to reinforce high-quality behaviors. In addition, during pairwise comparisons, we introduce the notion of *Preference Strength* (see Appendix A.4), categorizing preferences into “significant”, “moderate”, and “slight” differences, thereby providing the reward model with richer ordinal regression signals beyond binary labels.

To assess the impact of this fine-grained annotation scheme on model discrimination, we evaluate the RM performance across different clinical categories. As shown in Fig. 4, the model performance exhibits pronounced heterogeneity. For knowledge-intensive or relatively well-defined categories such as *Etiology* (0.74) and *Efficacy* (0.71), the model achieves higher correctness scores, suggesting a robust capture of factual medical knowledge. In contrast, categories

Table 5 | The Hexa-Dimensional Utility Framework (HDUF). This taxonomy decomposes utility into six measurable dimensions to guide fine-grained annotation and optimization.

Dimension	Definition
Relevance	Adherence to query constraints (e.g., format, steps, persona); accurate interpretation of user inquiry; direct resolution of query intent; absence of irrelevant or evasive content.
Logical Coherence	Direct response to the core requirements of the query; structural rationality of the overall framework; absence of logical gaps or internal contradictions.
Completeness	Comprehensive coverage of all essential points and key information required by the query.
Harmlessness	Absence of medium-to-high risk content or potential safety violations.
Helpfulness	Focus and conciseness of the content; provision of explicit and actionable conclusions.
Presentation Quality	Presence of introductory and concluding summaries; consistency and professional quality of the reading experience across sections.

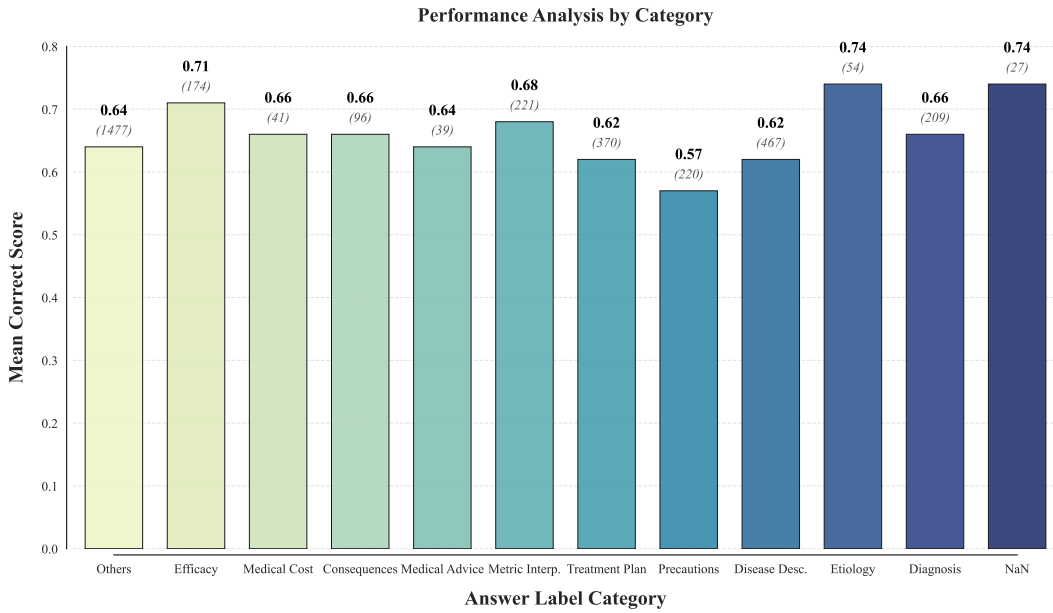


Figure 4 | Performance analysis across diverse medical categories, illustrating the heterogeneity in correctness scores.

that require nuanced clinical judgment and safety awareness—such as *Precautions* (0.57) and *Treatment Plan* (0.62)—pose significantly greater challenges. This observation reveals the current capability boundary of the RM: while it excels at factual recognition, it still requires stronger reasoning capacity to robustly assess the rigor of complex clinical decision-making and risk-sensitive guidelines.

3.2.2. Robust Training Strategies and Distribution Calibration

During the transition from annotated data to reward model training, we identify and address three core factors that undermine training stability: length bias, sample ambiguity, and gradient instability.

The first issue is the systemic conflict induced by *length bias*. Empirical evidence shows that annotator preferences regarding response length vary substantially across dimensions: correctness-oriented judgments favor conciseness, whereas completeness-oriented judgments favor verbosity. When naively mixed during training, the model easily falls into a spurious “longer-is-better” correlation. To mitigate this effect, we implement *Length-Aware Sample Balancing*, employing bucketed sampling strategies that force the model to attend to content quality rather than token count.

The second challenge concerns the utilization of *Tie/Same* samples. In medical scenarios, approximately 50% of response pairs are annotated as having no clear superiority. Traditional Bradley–Terry style reward models typically discard such samples, resulting in training sets dominated by easily distinguishable examples and weakening discrim-

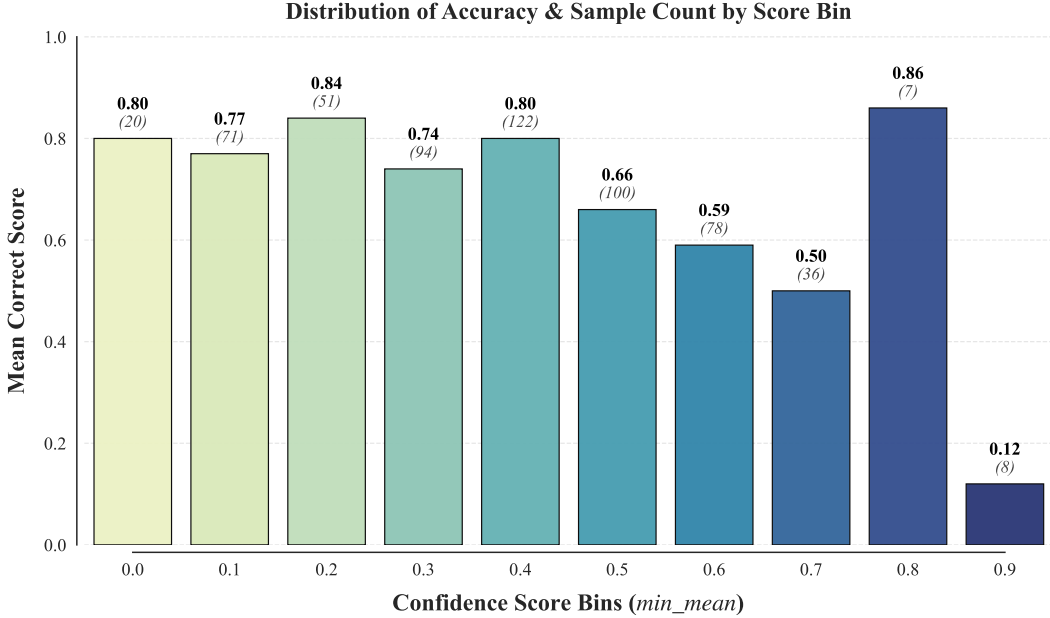


Figure 5 | Distribution of discrimination accuracy across score bins, illustrating a U-shaped trend with lower performance in the middle range.

ination near the decision boundary. We propose a *Margin-Constrained Loss* that explicitly models equivalence by minimizing the reward difference between Same pairs, i.e., $|r_\theta(y_1) - r_\theta(y_2)| \rightarrow 0$.

Finally, to address severe reward distribution fluctuations during early training—which may lead to gradient explosion—we replace fixed clipping thresholds with a *Dynamic Distribution Clamping* strategy. Based on real-time statistics of validation rewards (mean μ and standard deviation σ), we dynamically set clamping intervals (e.g., $[\mu - 2\sigma, \mu + 2\sigma]$). This approach suppresses extreme outliers while preserving informative tail behavior, thereby preventing gradient vanishing and avoiding catastrophic “training collapse”.

3.2.3. Experimental Evaluation and In-depth Attribution Analysis

To comprehensively evaluate the effectiveness of the proposed optimization strategies, we conduct detailed analyses across different score ranges and task types, and quantify the marginal benefits of data augmentation through ablation studies.

Score Range Sensitivity As illustrated in Fig. 5, we analyze RM discrimination accuracy across different predicted score intervals. The results exhibit a pronounced U-shaped distribution: the model achieves near-90% accuracy in both high-score (> 0.8) and low-score (< 0.2) regimes, while performance degrades noticeably in the mid-range ($0.4 \sim 0.6$). This indicates that the model can easily distinguish high-quality from poor-quality answers, but remains uncertain when differentiating between mediocre and barely acceptable responses. This finding motivates our subsequent active learning strategy, which prioritizes hard negative mining in the mid-score region.

Gains from Multi-turn Dialogue and Same Samples Given the multi-turn nature of medical consultations, we evaluate model performance under varying data scales and proportions of Same samples. As shown in Table 6, increasing the volume of multi-turn dialogue preference data (from 500 to 3.5k) yields steady improvements in both Macro-Average and SGS benchmarks, with no observable saturation, demonstrating the sustained benefits of the data flywheel.

Comparing *multiround_3500* with *multiround_3500_same_500*, the introduction of a moderate number of Same samples (~ 500) boosts the multi-turn dialogue metric from 76.65% to 79.64%, alongside an approximately 2% gain in R1-Macro. This confirms that learning “what is similar” helps the model more precisely define decision boundaries and, in turn, determine “what is better”. However, the gains are bounded: when the number of Same samples increases to 1000, performance degrades, with the multi-turn metric dropping to 74.56%, even below the baseline. This suggests that excessive Same samples dilute preference gradients. Accordingly, careful control of the mixing ratio between pairwise and pointwise signals is required, with empirical results recommending a ratio between 3:1 and 4:1.

Table 6 | Ablation study on multi-turn dialogue data scale and Same samples.

Configuration	R1 Macro-Avg	SGS Macro-Avg w/o Multi-turn	SGS Macro-Avg w/ Multi-turn	Multi-turn Dialogue	Historical Eval Sets	MACRO Average
baseline	61.32%	70.47%	69.37%	66.44%	68.45%	–
multiround_500	62.09%	69.96%	71.28%	74.82%	70.64%	71.16%
multiround_1000	59.44%	69.02%	70.42%	74.14%	68.62%	70.03%
multiround_2000	63.79%	68.51%	70.27%	74.95%	70.22%	71.54%
multiround_3500	62.76%	68.04%	70.39%	76.65%	71.15%	71.15%
multiround_3500_same_500	64.55%	66.81%	70.31%	79.64%	73.04%	71.85%
multiround_3500_same_1000	62.15%	67.50%	69.42%	74.56%	70.89%	70.52%
multiround_3500_same_2300	61.82%	68.85%	70.56%	75.12%	70.22%	71.52%

Table 7 | Ablation study of sampling strategies on the Precaution generation task.

Configuration	MACRO-Avg	R1-MACRO	SGS-MACRO
1000_pair	70.60%	63.55%	68.27%
1456_pair	70.62%	60.70%	68.40%
1456_balance_pair	71.91%	64.16%	68.36%
2030_pair	70.96%	63.68%	67.97%
1456_balance_same_500	70.98%	61.63%	69.00%
1456_balance_same_826	70.18%	62.03%	69.05%

Task-level Generalization We observe similar robustness gains on the **Precaution** generation task. As reported in Table 7, after balancing pairwise data (*1456_balance_pair*), the inclusion of Same samples (*1456_balance_same_826*) yields the highest SGS-Macro score of 69.05%. This further validates the generalization effectiveness of the mixed-sample strategy across diverse medical sub-tasks.

3.3. Expert Knowledge Alignment: A Dynamic Evaluation System Based on Automated Rubrics

In the high-risk vertical domain of medical question answering, general-purpose LLMs commonly suffer from the dual challenges of *knowledge hallucination* and *logical inconsistency*. To externalize implicit expert knowledge into executable supervision signals, we propose an *Automated Rubrics System*. This system constructs high-quality reference answers (Ground Truth, GT) through offline multi-model voting and DeepResearch, and decomposes them into four orthogonal evaluation dimensions: basic constraints, coverage completeness, knowledge density, and factual consistency. Building upon this foundation, we design a non-linear scoring mechanism incorporating normalization, saturation clipping, and dynamic scaling. Combined with knowledge distillation, this approach effectively mitigates sparsity, robustness, and inference latency issues inherent in traditional rule-based scoring.

3.3.1. Rubric Generation

High-quality rubrics originate from precise medical facts. To address the long-tail and high-complexity characteristics of medical queries, we design an *Adaptive GT Generation Pipeline*, as illustrated in Fig. 6, covering the entire process from multi-perspective sampling to evidence reconstruction.

For simple medical queries, we assume that state-of-the-art models (e.g., GPT-5.2 (OpenAI, 2025), Qwen3-Max (Yang et al., 2025a), Gemini3-Pro (Google DeepMind, 2025)) exhibit high consensus. Accordingly, we adopt a *Multi-Model Ensemble Sampling* strategy, constructing prompts with diverse styles (e.g., “in-depth analysis”, “concise explanation”, and “layman-friendly interpretation”) to induce diversified responses. Consensus knowledge points are then extracted via clustering algorithms to form the GT backbone.

In contrast, for complex and difficult queries, substantial inter-model disagreement is often observed. To handle this, we introduce a *Difficulty Detection* mechanism based on cross-scoring to compute an inter-model consistency

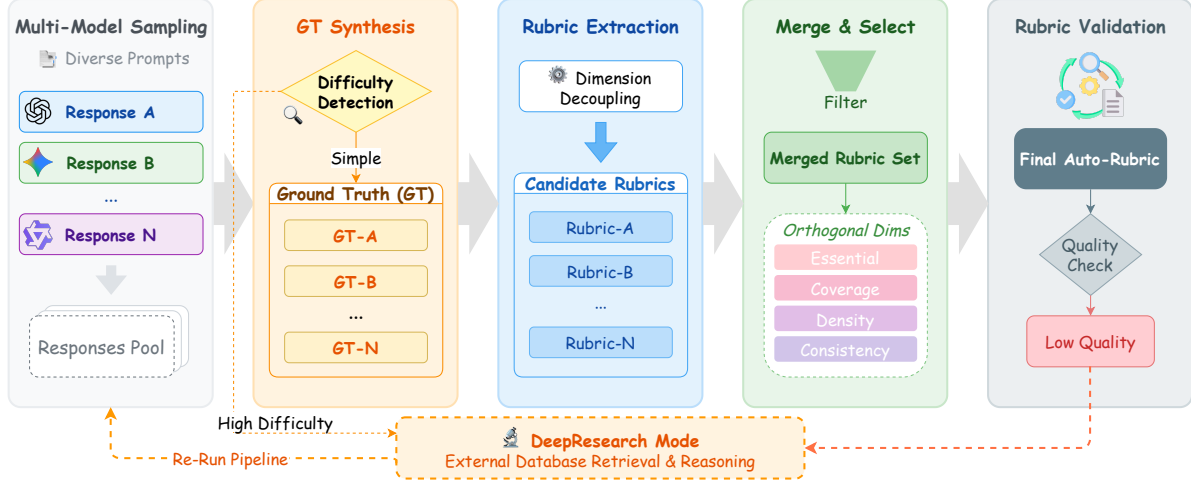


Figure 6 | Pipeline of automated rubric generation. The process integrates multi-model sampling, consensus-based GT synthesis, and DeepResearch-driven refinement for complex medical queries.

coefficient. When the consistency falls below a predefined threshold, the system automatically triggers a DeepResearch mode, invoking external authoritative medical databases for multi-hop reasoning and evidence retrieval. Guided by the latest clinical guidelines, a high-quality GT grounded in evidence-based medicine is reconstructed. This closed-loop “detect–retrieve–reconstruct” pipeline ensures both the authority and timeliness of the rubrics.

3.3.2. Hierarchical Rubric System Construction

To comprehensively capture the quality characteristics of medical responses, a single-dimensional scoring criterion is insufficient. Therefore, based on automated GT, we construct an orthogonal and complementary *Hierarchical Rubric System*, composed of four sub-rubrics that jointly audit model outputs from multiple granularities.

Basic Rubrics Basic rubrics form the foundation of the evaluation system, focusing on instruction-following capability and role consistency. We define four core scoring categories: *Essential*, which specifies mandatory knowledge points and establishes the logical lower bound of a response; *Important*, which covers professional explanations required for high-quality answers; *Extension*, which rewards beyond-expectation depth and potential need fulfillment; and *Pitfall*, which serves as a negative reinforcement signal to identify potential risks. This module primarily verifies compliance with prompt constraints (e.g., bullet-point formatting) and prohibitions (e.g., avoiding diagnosis), ensuring basic validity and normativity of model outputs. A representative example of such rubrics is illustrated in Appendix B.

Comprehensive Rubrics via Checklists To assess both depth and breadth, we construct high-granularity comprehensive rubrics based on checklists. The unstructured GT is decomposed into multiple knowledge topics and their associated atomic points, enabling fine-grained coverage of the knowledge topology. These points are mapped to three progressive cognitive attributes: *Essential*, covering core medical facts (e.g., diagnostic criteria, first-line medications) and defining the passing threshold; *Highlight/Aha*, emphasizing deeper exploration of latent user needs (e.g., pathophysiological explanations, evidence-based justification), reflecting expert-level insight; and *Extension*, evaluating derivative recommendations beyond the core demand (e.g., lifestyle interventions, operational guidance) to enhance utility breadth and humanistic care. This layered design guides the model from merely “answering correctly” toward “answering thoroughly and insightfully.” An illustrative example of such a rubric is provided in Appendix C.

Knowledge Density Rubrics During early reinforcement learning experiments, we observe a pronounced reward hacking phenomenon: as basic and comprehensive rubrics favor recall of knowledge points, models tend to exploit verbosity by generating long, repetitive, or circular responses to trigger keyword matches. To counteract this length bias, we introduce knowledge density rubrics. Inspired by the concept of *Key Tokens* (Wang et al., 2025), we design an entropy-based density constraint. The system first extracts condensed *Key Information Units* (*KIUs*) from the GT, such as salient entities, action verbs, and critical numerical values. It then computes the number of unique *KIUs* per unit length in the generated response. This metric is used as a penalty term to aggressively suppress low-density verbosity, forcing the model to pursue concise yet information-rich expression. An illustrative example of the knowledge density rubric is provided in Appendix D.

Correctness Rubrics To enforce the medical safety boundary, we design Correctness Rubrics as a circuit breaker for the entire evaluation system. This dimension consists of two core checks: *Conflict Detection*, which identifies logical contradictions between the response and the core facts defined in basic or comprehensive rubrics (e.g., recommending a medication and later listing it as contraindicated); and *Error Mining*, which leverages historical rollout data and errors accumulated during retrieval-augmented processes to maintain a dynamically updated “negative knowledge base.” This module specifically checks whether the model violates common cognitive pitfalls or clinical contraindications. Detection of such high-risk information triggers penalties that directly reduce the final score.

Table 8 | Ablation study: Impact of different weight configurations on ranking accuracy.

Setting	Essential : Important : Extension : Penalty	Positive/Negative Ratio
Uniform (Baseline)	1:1:1:1	2:1
Increased Ess. & Pen. weights	2:1:1:2	3:1
Further increased Ess. & Pen. weights	3:1:1:3	Slightly less than 3:1
Differentiated Imp. & Ext. weights	3:2:1:3	Slightly greater than 3:1

3.3.3. Non-linear Scoring Mechanism

In open-ended QA settings, where answer quality lacks a strict upper bound, evaluation should emphasize relative ranking rather than absolute scores. Accordingly, we adopt a tiered ranking approach inspired by *Bucket Sort*. By constructing multi-level, multi-type buckets, responses of varying quality are structurally grouped. This bucketing mechanism calibrates partial order relations among scores, ensuring that evaluation outcomes accurately reflect relative model capabilities.

Normalization and Differentiated Weighting Given the heterogeneous numeric scales across rubric dimensions, we first apply min–max normalization to map all indicators into the $[0, 1]$ range. For final aggregation, differentiated weighting is required to faithfully reflect response quality. We construct multiple weight configurations and validate them via A/B testing on manually annotated pairwise samples. By analyzing changes in the positive-to-negative ranking ratio, we observe that increasing the weights of *Essential* and *Pitfall* significantly improves ranking accuracy (from approximately 2:1 to 3:1). Based on the ablation results in Table 8, we adopt the weight scheme:

$$\text{Essential : Important : Highlight : Pitfall} = 2 : 1 : 1 : 2.$$

The weighted scoring function is defined as:

$$\text{Score} = \frac{\sum_{i \in \{\text{essen, ext, aha}\}} \sum S(\text{Res}, R_i) - \sum S(\text{Res}, R_{\text{pit}})}{\sum_{i \in \{\text{essen, ext, aha}\}} \sum R_i - \sum R_{\text{pit}}}. \quad (1)$$

Here, $\{\text{essen, imp, ext}\}$ denote positive indicators, while R_{pit} represents penalty items. This formulation ensures that safety and core factual correctness dominate auxiliary information, effectively improving the positive/negative ranking ratio from 2:1 to 3:1.

Saturation and Length Adversarial Mechanisms To prevent score inflation through redundant verbosity, we introduce a *Saturation* mechanism. For *Important* and *Highlight* items, an upper bound L is imposed to cap score accumulation:

$$S_{\text{imp, aha}} = \min \left(\sum_{i \in \text{Tags}} \min \left(\sum S(\text{Res}, R_i), L \right), 2 \sum S(\text{Res}, R_{\text{essen}}) \right),$$

$$\text{Tags} = \{\text{Imp, Aha}\} \parallel \{\text{InfoQual, EvidenSup, Safety, Read, HumCare}\}.$$

To operationalize the knowledge density rubric, we further introduce an information-density-based length adversarial term S_{balance} . By computing the ratio between effective knowledge phrases $|R_{\text{phrase}}|$ and total response length $\text{len}(\text{Res})$, we apply a non-linear penalty to low-density text:

$$S_{\text{balance}} = \frac{\sum \text{Score}(\text{Res}, R_i)}{\text{len}(\text{Res}) / |R_{\text{phrase}}|}.$$

Dynamic Scaling and Activation To provide sharper gradient signals during reinforcement learning and encourage capability extrapolation, we propose a *Dynamic Scaling* strategy. Specifically, we compute the mean score S_{mean} of several strong reference models under the same input as a dynamic baseline. When a rollout response achieves $S_{\text{roll}} > S_{\text{mean}}$, the surplus reward is amplified via a scaling factor W_{scale} , thereby enlarging the reward margin between outperformers and mediocre samples:

$$S_{\text{scale}} = \begin{cases} S_{\text{roll}}, & S_{\text{roll}} < S_{\text{mean}}, \\ S_{\text{mean}} + W_{\text{scale}} \cdot (S_{\text{roll}} - S_{\text{mean}}), & S_{\text{roll}} > S_{\text{mean}}. \end{cases}$$

The baseline mean is defined as the arithmetic average over N reference models:

$$S_{\text{mean}} = \frac{\sum_{i \in \{GPT, R1, Qwen, \dots\}} S_i}{N}$$

3.3.4. Performance Evaluation and Online Parallel Scoring

To validate both the effectiveness and engineering feasibility of the rubric-based scoring system, we analyze the positive-to-negative ranking ratio on pairwise samples in the test set. As shown in Table 9, the results reveal pronounced performance heterogeneity. The system excels at capturing relevance and completeness, with ranking ratios reaching 4.74 for “severe intent deviation” and 3.3 for “missing core dimensions”, demonstrating strong sensitivity to major quality gaps. However, effectiveness degrades notably for formatting conventions and deep logical consistency: low ratios for “poor textual formatting” (0.67) and “internal viewpoint conflict” (0.5) indicate that rubrics alone cannot fully cover all evaluation dimensions and must complement other reward models.

To meet the stringent low-latency requirements of large-scale RL training, we adopt a rubric-splitting and parallel scoring strategy. By distilling the scoring capability into a Qwen3-8B model via supervised fine-tuning, we successfully reduce end-to-end scoring latency to under 200 ms, achieving high-throughput real-time feedback while maintaining evaluation fidelity.

Table 9 | Analysis of Positive/Negative Ranking Ratios across different error categories.

High Discrimination		Moderate Discrimination		Low Discrimination	
Error Category	Ratio	Error Category	Ratio	Error Category	Ratio
Severe Intent Deviation	4.74	Counterfactual Failure	1.60	Insufficient Normativity	0.67
Partial Intent Deviation	3.17	TCM/WM Misalignment*	1.50	Local Logical Incoherence	0.594
Core Dim. Missing	3.30	Poor paragraph Relevance	1.25	Internal Contradiction	0.50
Partial Dim. Missing	2.61	Medical Risk	1.25	Paragraph Redundancy	0.417
Important Dim. Missing	2.138	No Introductory Summary	1.00	Poor Cohesion	0.25
No Concluding Summary	2.00	Core Argument Conflict	1.00	Minor Word Repetition	0.33

Note: The Ratio is defined as the ratio of correctly ranked pairs (positive) to incorrectly ranked pairs (negative). It characterizes the discriminative power of the reward model across various error categories.

* TCM/WM refers to the inappropriate mixing of Traditional Chinese Medicine and Western Medicine.

3.4. User Feedback Alignment: Reward Modeling for Sparse and Noisy Online Signals

Traditional RLHF paradigms rely heavily on expert annotations. However, expert feedback often suffers from substantial latency and fails to capture the diverse, subjective, and dynamically evolving user needs in real-world production environments. Meta’s experiments (Han et al., 2025) demonstrate that large-scale, timely binary user signals (such as “Like” or “Love”) exhibit a strong correlation with long-term user retention (Pearson $r = 0.95$), highlighting their significant potential as reward signals. Nevertheless, directly optimizing with sparse and noisy point-wise user feedback poses severe challenges. Such feedback is inherently sparse and high-variance: user likes are frequently influenced by transient emotions, stylistic preferences, contextual expectations, or even random factors, resulting in a misalignment between observed rewards and true user-perceived usefulness. Naively maximizing the probability of “Like” ($P[\text{Like}]$) leads to pronounced capability trade-offs. While the tone becomes more amiable, the “Helpfulness” score drops from

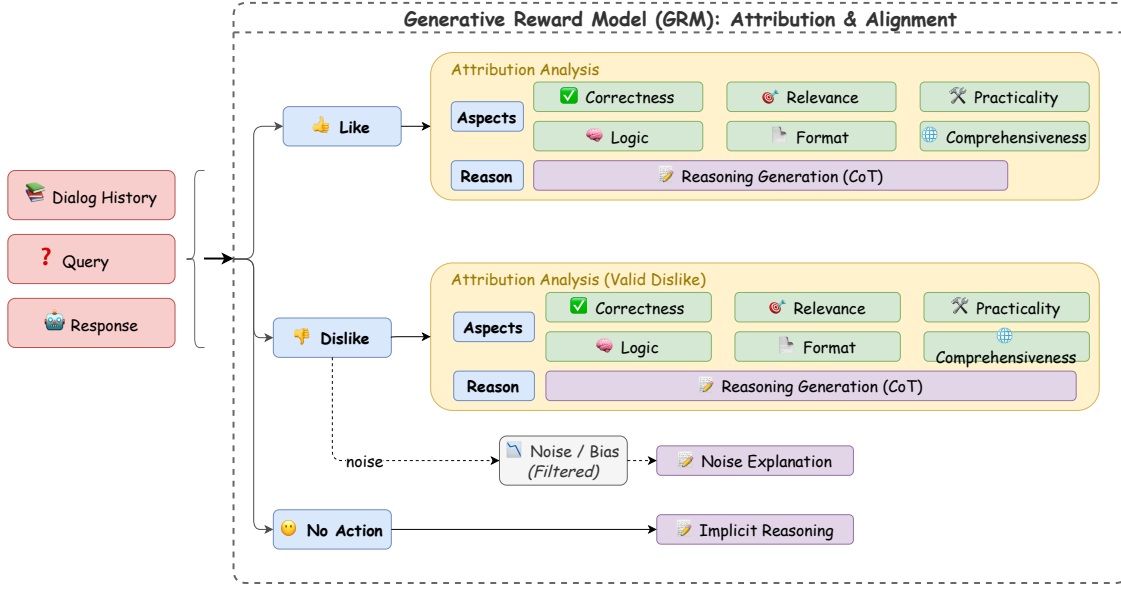


Figure 7 | Architecture of the Generative Reward Model (GRM) featuring multi-dimensional attribution.

-4% to -16% . More critically, models exhibit clear reward hacking behaviors: to elicit positive feedback, the model may prematurely terminate conversations or excessively overuse farewell expressions such as “Bye!”, with frequencies increasing up to four times the baseline.

To address these challenges, we reformulate traditional discriminative, point-wise scalar regression for reward learning into a GRM paradigm that follows a “first attribute, then label” strategy. Conditioned on the dialogue history, query, and response, the model generates structured attribution analyses spanning correctness, logical coherence, relevance, completeness, utility, and presentation, which are then used to denoise and calibrate like/dislike signals while improving interpretability. Furthermore, by integrating RMBoost-style end-to-end pair construction and length-balancing strategies, we transform sparse and noisy point-wise feedback into high-quality pair-wise preference data and optimize them robustly using the Bradley–Terry model, thereby achieving more reliable alignment with true user satisfaction.

3.4.1. Attribution-Driven Generative Reward Modeling for Noisy Feedback

To effectively address noise in user feedback—our random sampling analysis indicates that the behavioral rationality of “Like” samples reaches 96%, whereas “Dislike” samples drop to only 76%—we reformulate reward modeling as a generative task. As illustrated in Fig. 7, we propose a GRM that leverages the Chain-of-Thought (CoT) reasoning capability of LLMs. Instead of directly outputting scalar rewards, the model first produces structured attribution analyses and subsequently predicts the final label.

To enable fine-grained attribution, we define a taxonomy comprising six major dimensions, as summarized in Table 10. This framework spans from fundamental correctness to higher-level utility, allowing the model to precisely identify defects that lead to user “Dislike” (e.g., factual errors or logical contradictions) as well as drivers of “Like” (e.g., comprehensive coverage).

Introducing CoT reasoning substantially improves the robustness and interpretability of reward signals. As shown by the ablation results in Table 11, the “reason-first” strategy (*qwen3_reverse*) outperforms the non-CoT baseline by a large margin, particularly increasing the Overall Accuracy from 0.485 to 0.610. This mechanism forces the model to perform explicit reasoning before decision-making, which is evidenced by the significant jump in positive sample (Like) F1-score to 0.687, representing a substantial gain in preference detection reliability.

3.4.2. Pairwise Preference Construction and Optimization via Attribution Denoising and Data Augmentation

Given the sparsity of online feedback, directly collecting multiple responses of varying quality for the same query is extremely challenging. To enable more stable pair-wise preference optimization algorithms (e.g., the Bradley–Terry model), we design a data augmentation pipeline inspired by RMBoost. As illustrated in Fig. 8, the pipeline first applies GRM-based attribution denoising to online data, followed by synthetic pair construction through reverse modification

Table 10 | Attribution taxonomy for multi-dimensional feedback analysis and defect localization.

Dimension	Issue Type
Correctness	Factual inaccuracies, improper terminology, lack of rigor, ambiguity, numerical errors, computational mistakes, and common-sense errors.
Logical Coherence	Verbosity, overlapping or redundant points, suboptimal ordering (failure to prioritize key points), and internal inconsistencies or contradictions.
Presentation	Typos, grammatical errors, improper punctuation, poor segmentation, content truncation, ineffective use of tables, and poor overall readability.
Relevance	Irrelevant sentences, detachment from dialogue context, thematic deviation, or off-topic responses.
Completeness	Omission of essential dimensions or insufficient elaboration on critical points.
Utility	Inadequate diagnostic orientation, ambiguous perspectives, lack of department or medication guidance; poor practical feasibility, lack of focus, or failure to integrate user-specific constraints.

Table 11 | Performance comparison of Reward Model strategies across different CoT reasoning patterns.

Model	Aspect Acc	Overall Acc	Label	Performance			Interpretability Pattern & Example
				Precision	Recall	F1	
qwen3_no_cot	0.520	0.485	like	0.583	0.067	0.120	No CoT: Direct label generation. [Like/Dislike, Comprehensive: Good/Poor]
			dislike	0.479	0.947	0.636	
			Macro-F1	--	--	0.378	
qwen3_cot	0.560	0.580	like	0.598	0.610	0.604	CoT: Label first, then explain. [Like/Dislike, ..., Reason: xxx]
			dislike	0.559	0.547	0.553	
			Macro-F1	--	--	0.578	
qwen3_reverse	0.575	0.610	like	0.564	0.876	0.687	Reverse CoT: Explain first, then label. [Analysis: xxx, Therefore: Like/Dislike]
			dislike	0.588	0.316	0.411	
			Macro-F1	--	--	0.549	

and resampling strategies.

As shown in Fig. 9, *reverse modification* uses GRM-identified strengths or weaknesses to guide an LLM to rewrite the original response by degrading strengths or correcting weaknesses, whereas *temperature-based resampling* generates multiple responses across different model versions by varying the sampling temperature. All constructed pairs are automatically validated using an “LLM-as-a-Judge” mechanism.

To assess data quality, we compare sample pairs containing real user behavior (External) with purely synthetic pairs (Internal). As reported in Table 12, External pairs achieve an accuracy of 92%, significantly outperforming Internal pairs at 83%, underscoring the importance of preserving genuine user signals. Moreover, to mitigate potential length bias—as “Like” samples tend to be longer—we apply length-balancing during sampling, effectively reducing overfitting to response length.

3.4.3. Experimental Results and Analysis

We conduct comprehensive evaluations through offline benchmarks and large-scale online A/B tests. Offline results, summarized in Table 13, show that the Uni-Normalize strategy incorporating user feedback significantly outperforms the SFT baseline across key metrics such as honesty, relevance, and comprehensiveness. Importantly, it maintains reasonable response lengths, avoiding excessive verbosity.

Finally, online A/B bucket experiments validate the practical value of the proposed approach. As shown in Table 14, the experimental bucket achieves a 9.72% increase in completion rate (a proxy for user retention), a 5.56% improvement in UV like/dislike interaction rate, and a higher proportion of likes. These results demonstrate that transforming high-noise, point-wise online feedback into interpretable, high-quality pair-wise signals via GRM effectively bridges the

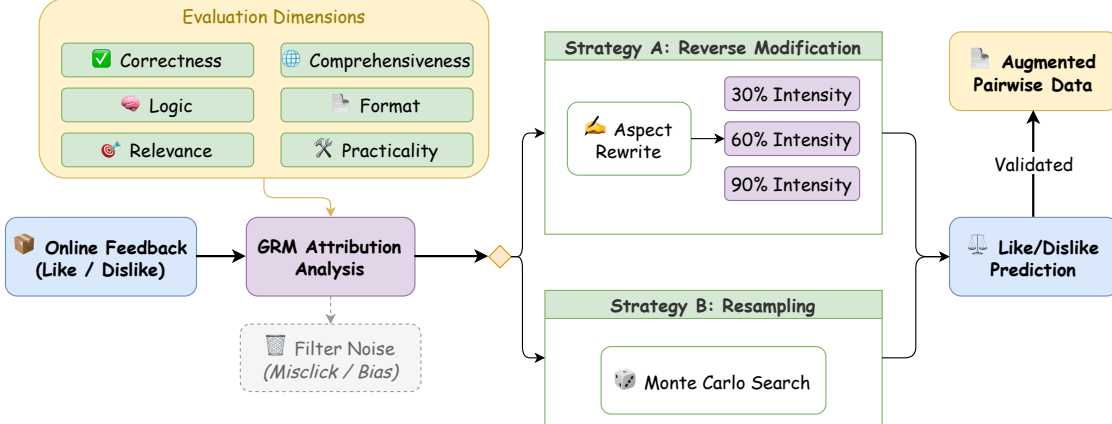


Figure 8 | Architecture of the attribution-based pairwise data augmentation pipeline.

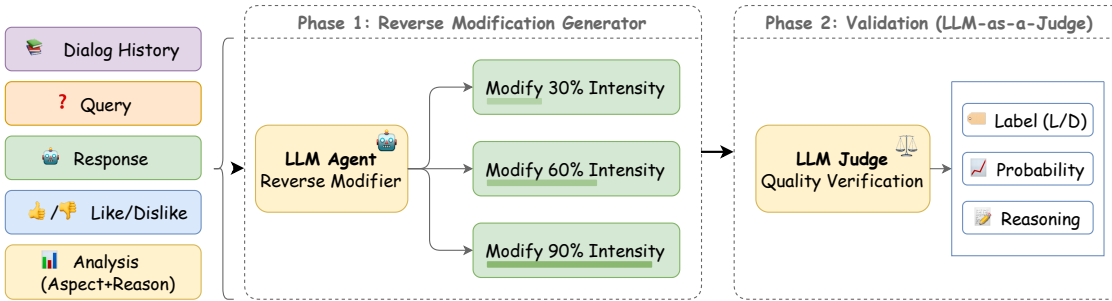


Figure 9 | Two-phase pipeline for pairwise data construction via reverse modification and LLM-as-a-Judge validation.

gap between offline training objectives and real user satisfaction.

3.5. Format Alignment: Highlighting, Tabulation, and Authority Citation

In medical QA scenarios, the form of information presentation directly correlates with user cognitive load and the establishment of trust. To enhance the readability and professionalism of responses, we constructed a multi-dimensional format alignment strategy, focusing specifically on **Highlighting & Tabulation** and **Authority Citation**. Our workflow follows a two-stage paradigm of “Capability Verification → Strategy Optimization”: first, we endow the model with fundamental format discrimination and generation capabilities via SFT; subsequently, we leverage RL strategies to unleash the model’s generation potential in actual deployment, significantly improving the coverage and accuracy of formatted content.

3.5.1. *Highlighting and Tabulation: RL-Based Optimization for Structured Generation*

Structured representations, such as tabular comparisons and key-point highlighting, significantly enhance the clarity of complex medical information. However, a fundamental challenge for LLMs remains the *generative timing*—recognizing not only how to construct these formats but also when to trigger them contextually.

Discriminative Capability Verification To ensure the reliability of model generation, we first defined “whether to generate a chart/table” as a binary classification problem based on the Title + Content context. We conducted specialized SFT on the Qwen3-8B base model and evaluated its discriminative quality using a strict test set. As shown in Table 15, the model performed excellently in both table and image generation discrimination tasks. Particularly for image generation, the model achieved a Precision of 100.00% and an F1 score of 97.14%, demonstrating its ability to accurately judge whether the current semantics are suitable for multi-modal content generation. The F1 score for table generation also reached 87.27%, providing a solid discriminative foundation for subsequent RL optimization.

RL-Driven Coverage Enhancement Despite the high precision of the discriminative model, we observed in actual deployment that the model tended to be conservative during online inference, resulting in a lower-than-expected trigger rate for structured content. To address this, we introduced reinforcement learning training to adjust the model’s

Table 12 | Accuracy and length distribution of constructed pairs across user behavior and data source dimensions.

Comparison Dimension	Pairwise Accuracy	Fitting Rate	Length Preference (Ratio [Mean])	
User Behavior Dimension Analysis				
User Like	59 : 5	49 : 10	64 : 0	(650 : 400)
User Dislike	33 : 3	30 : 3	12 : 21	(517 : 537)
Data Source Comparison (External vs. Internal)				
External vs. Internal	83 : 17	79 : 4	69 : 31	(567 : 434)

Table 13 | Offline performance comparison between the baseline and proposed alignment schemes.

Alignment Scheme	Honesty ↑	Relevance ↑	Comp. ↑	Length ↓
Baseline	0.770	0.940	0.165	424.6
Uni-Normalize Scheme	0.830	0.935	0.225	573.1
Uni-Normalize Scheme + Like/Dislike Helpful RM	0.779	0.940	0.206	412.0

generation tendency by optimizing the Reward strategy. Specifically, we designed a targeted reward function to encourage the model to actively output structured content in scenarios deemed “suitable for generation” while penalizing format abuse. Experimental results show that, while maintaining high precision and recall, the RL strategy significantly improved business coverage: image generation coverage jumped from 3% to 12%, and table generation coverage increased from 1% to 3%. This significant growth validates the effectiveness of RL in unleashing model potential and balancing “conservative” versus “active” strategies.

3.5.2. Authority Citation: Building a Trustworthy Medical Attribution System

In Medical QA, factual correctness alone is insufficient for establishing clinical trust. To mitigate “Hallucination of Attribution”—characterized by fabricated citations or misinterpreted evidence—we prioritize **Authority Citation** as a core architectural objective. This paradigm requires the model to synthesize high-grade evidence (e.g., clinical guidelines and seminal textbooks) and provide references via standardized syntax (e.g., superscripts). This approach enhances both professionalism and interpretability. To this end, we propose a two-stage optimization framework integrating “Metadata-Driven Instruction Tuning (SFT)” and “Rule-Guided Policy Optimization (RL)”, achieving high-precision medical attribution without compromising conversational fluency.

Metadata-Driven Instruction Tuning The acquisition of authority citation capability begins with high-quality supervisory signals. In early experiments, we found that relying solely on raw unstructured RAG documents made it difficult for the model to effectively distinguish the weight differences between “general popular science articles” and “core clinical guidelines” in the latent space, leading to highly random citation behaviors. Consequently, we designed a structured data construction pipeline to reconstruct traditional flat contexts into structured objects containing rich metadata. As shown in Figure 10, each retrieved segment is assigned explicit labels such as *Authority Level* (e.g., Level A/B/C, where Level A corresponds to authoritative guidelines/textbooks), *Source Name*, and *Publication Date*. By introducing an “Instruction Isolation” mechanism in the System Prompt, we force the model to prioritize Level

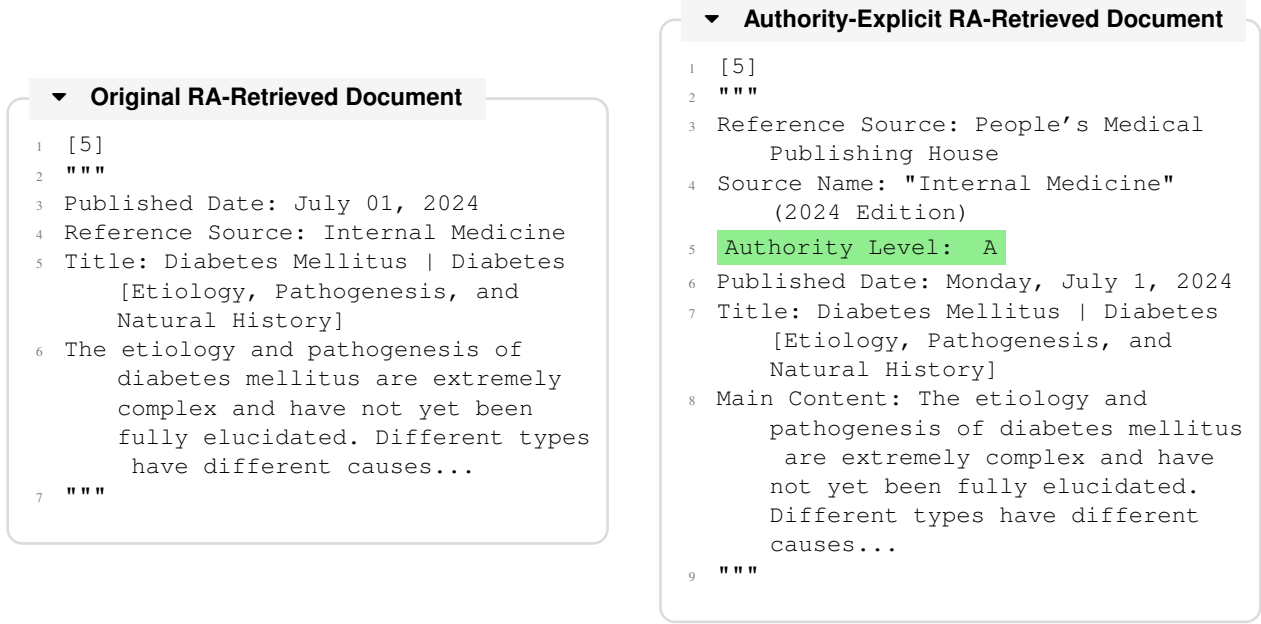
Table 14 | Online A/B testing results comparing baseline and experimental groups across core business metrics.

Group (Bucket)	Completion Rate ↑	Query Reform. Rate ↓	Interaction Rate (UV) ↑	Positive Feedback Ratio (UV) ↑
Baseline	63.96%	28.11%	1.33%	57.14%
Experimental	70.18%	28.11%	1.41%	58.46%
Relative Improvement	+9.72%	—	+5.56%	+2.31%

Table 15 | Performance of the format discrimination model for table and image generation.

Task Category	Accuracy	Precision	Recall	F1 Score
Table	85.57% (83/97)	88.89% (48/54)	85.71% (48/56)	87.27%
Image	97.00% (97/100)	100.00% (51/51)	94.44% (51/54)	97.14%

Figure 10 | Comparison of RAG input formats: original versus metadata-enriched authority-explicit context.



A evidence during generation and ignore low-confidence information. This explicit feature injection provides clear *Attention Anchors* for the model.

To investigate the impact of data scale, we conducted an ablation study to identify the critical threshold for effective citation learning. As shown in Table 16, results reveal a distinct scaling effect: with fewer than 500 samples, citation behavior remains inconsistent (rate < 37%), suggesting a failure to acquire syntactic patterns. Conversely, increasing the dataset to 1,000 samples boosts the citation rate to 76.30%, with diminishing returns thereafter. Guided by this, we curated a golden set of ~1,000 samples subject to rigorous human verification. By targeting long-tail errors such as improper placement and attribution inaccuracies, we established a robust performance baseline with minimal annotation cost.

Rule-Guided Policy Optimization Despite acquiring preliminary citation awareness through SFT, the model remains susceptible to robustness issues in open-ended scenarios, including hallucinated citations, malformed formatting, and over-citation (i.e., forced citations for irrelevant queries). To address these challenges, we implemented an efficient Rule-Based Reward Mechanism. We observe that for rigid constraints like citation formatting, heuristic rules—such as regular expressions and string matching—often offer stronger inductive bias and determinism than neural reward models, thereby providing clearer optimization signals. As illustrated in Figure 11, we formulate the discrete reward function R_{rule} as follows:

$$R_{rule}(y) = \mathbb{I}_{fmt}(y) + \mathbb{I}_{gold}(y) - \sum_{k \in \mathcal{K}} \mathbb{I}_{err_k}(y) \quad (2)$$

where \mathbb{I}_{fmt} rewards adherence to the standard format (e.g., «Title» (Year)), and \mathbb{I}_{gold} encourages alignment with sources in the gold standard document set. Conversely, \mathcal{K} represents a set of penalized error types, including incorrect source names, non-gold source citations, and repetition. The training dynamics presented in Table 17 demonstrate the effectiveness of this strategy: at step 100, citation coverage was merely 31.18%; by step 700, under explicit rule guidance, coverage rose to 60.21%, while accuracy reached 96.42%. These results suggest that establishing a baseline capability via SFT, followed by high-precision behavior shaping through rule-based rewards, constitutes a robust and efficient

Table 16 | Ablation study of SFT data scale on the performance phase transition of authority attribution.

Training Set Size	Cases of Explicit Authority Attribution in Test Set (Count & Ratio)
200	182 cases (16.85%)
500	395 cases (36.57%)
1000	824 cases (76.30%)
1500	725 cases (67.13%)
1700	814 cases (75.37%)

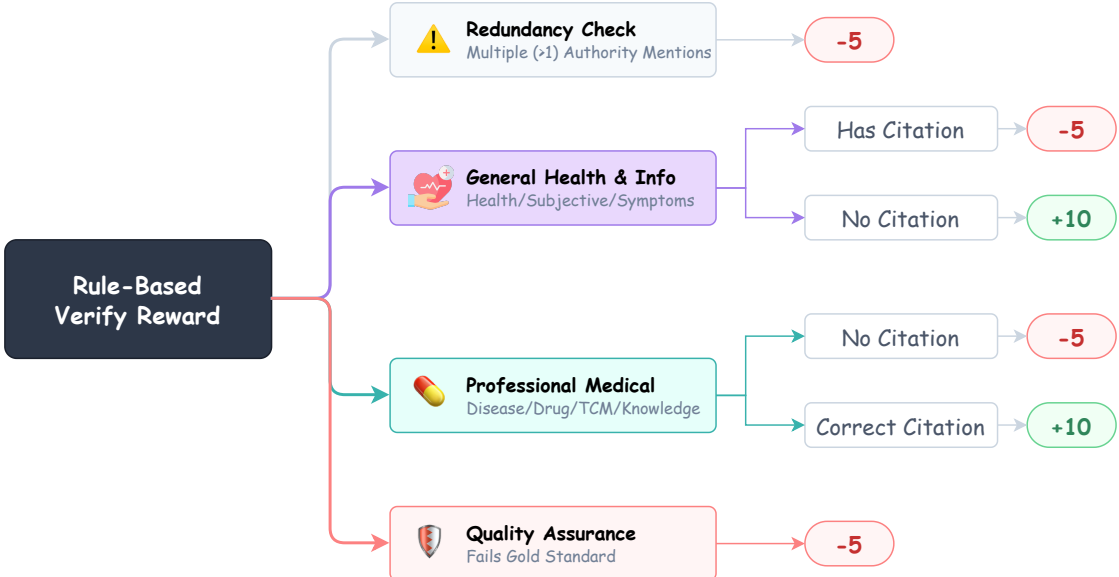


Figure 11 | Logic and scoring criteria of the rule-based reward for authority citation.

training paradigm.

4. Uni-Reward: Robust Multi-Objective Collaborative Optimization via Adaptive Modulation

In RL alignment for Medical QA, we formulate policy optimization as a Multi-Objective Markov Decision Process and construct a heterogeneous reward space \mathcal{R} composed of rule-based hard constraints, multi-dimensional reward models, and expert knowledge rubrics. However, directly optimizing such mixed objectives poses severe challenges. Reward signals from different sources (e.g., discrete rule-based 0/1 signals versus continuous RM logits) exhibit substantial distributional discrepancies, leading to pronounced scale mismatch, which in turn causes gradient domination and masking effects. Meanwhile, models tend to prioritize optimizing low-entropy surface features (e.g., formatting) while neglecting high-entropy clinical reasoning, resulting in endogenous optimization competition and reward hacking. To identify Pareto-optimal solutions under complex medical constraints, we propose the Uni-Reward framework. Uni-Reward first establishes a unified metric manifold via stationary distribution normalization. On this foundation, we systematically investigate and compare two dynamic weighting paradigms: control-theoretic Equal Contribution Collaborative Optimization (ECCO) and semantically aware Tri-Factor Adaptive Dynamic Weighting (TADW).

Table 17 | Ablation study of rule-based reward configurations on citation coverage and accuracy across training steps.

Reward Weight	Step	Coverage Rate (%)	Accuracy (%)
Setting A: Basic Rule Reward			
Rewards: Correct Name (+1), From Gold Doc (+1). Penalties: Wrong Name (-1), Not Gold Doc (-1), Repetition (-1), Hallucination (-1).			
1	400	45.16	88.09
	450	54.83	80.39
	500	41.93	89.47
	550	30.10	85.71
	600	46.23	86.04
	650	63.44	83.05
	700	64.51	85.00
	750	45.16	90.47
	400	49.46	78.26
3	450	40.86	86.84
	500	40.86	86.84
	550	48.38	88.88
	600	41.93	82.05
	650	63.44	87.93
	700	52.68	85.10
	750	52.68	79.59
	400	49.46	78.26
	450	40.86	86.84
Setting B: Enhanced Rule Reward (+ Source Attribution)			
Includes all rules from Setting A, plus reward for <i>Accurate Attribution Source</i> .			
1	100	31.18	82.14
	150	35.48	90.90
	400	50.53	82.97
	450	43.01	90.90
	500	40.86	91.89
	550	54.83	95.91
	600	45.16	97.61
	650	55.91	96.15
	700	60.21	96.42
	750	32.25	90.00
800			
46.23			

4.1. Stationary Distribution Normalization

When adopting GRPO for policy alignment, the primary obstacle to collaborative optimization lies in scale mismatch among heterogeneous reward signals. Although GRPO mitigates variance issues of a single reward function by computing intra-group relative advantages, in multi-objective settings we must first aggregate multiple heterogeneous reward signals (e.g., discrete Rubrics 0/1 indicators and continuous ORM logits) into a total reward R_{total} . If aggregated directly, reward components with larger numerical ranges dominate the overall distribution, causing numerically smaller yet critical signals to suffer from *gradient masking*.

Moreover, while online normalization is commonly used to standardize inputs, during early training stages the rapid evolution of policy π_θ induces drastic fluctuations in reward distribution statistics (mean and variance). This non-stationarity introduces covariate shift, destabilizes the optimization objective, and leads to oscillatory policy updates.

To address this issue, we propose **Reference-Frozen Normalization**, aiming to construct an absolutely stable metric baseline. Specifically, before GRPO training starts (Step $t = 0$), we perform large-scale Monte Carlo rollouts using the supervised fine-tuned policy π_{sft} on a validation set \mathcal{D}_{val} , yielding an initial trajectory set $\mathcal{T}_{\text{init}}$. Based on this

set, we obtain unbiased estimates of the fixed mean μ_k and standard deviation σ_k for each reward component r_k . For all subsequent training steps $t > 0$, these frozen statistics are used to map the raw reward outputs $\hat{r}_k^{(t)}$ into a standard normal space via the following Z-score transformation:

$$\tilde{r}_k(s, a) = \text{Clip}\left(\frac{\hat{r}_k(s, a) - \mu_k}{\sigma_k}, -\delta, \delta\right), \quad (3)$$

where δ is a truncation threshold (e.g., $\delta = 5.0$) to filter extreme outliers. This static transformation ensures that all reward components are projected onto a unified scale prior to aggregation, eliminating scale bias and providing an unbiased and stationary foundation for subsequent dynamic weighting.

4.2. Equal Contribution Collaborative Optimization (ECCO)

Within the unified scale space, we first explore a feedback-control-based dynamic modulation strategy ECCO to address multi-objective competition. ECCO is built upon a strong assumption: to avoid overfitting to any single dimension (reward hacking), all selected reward signals should maintain equal contribution to the overall optimization objective. We formalize this intuition as an online error minimization problem by dynamically adjusting the weight coefficients $\lambda_k(t)$, forcing the actual contribution ratios of all components to converge toward a predefined equilibrium target.

4.2.1. Error Feedback and Constrained Update

Let $\bar{r}_k(t)$ denote the batch-wise mean of the k -th reward component at step t . The actual contribution ratio is defined as:

$$P_k(t) = \frac{\lambda_k(t) \cdot \bar{r}_k(t)}{\sum_{j=1}^K \lambda_j(t) \cdot \bar{r}_j(t)}. \quad (4)$$

To drive $P_k(t)$ toward the target ratio P_{target} (typically set to $1/K$), we introduce an instantaneous error term $E_k(t) = \alpha \cdot (P_k(t) - P_{\text{target}})$ and update the weights via a first-order gradient descent rule. However, due to the stochasticity of RL training, unconstrained updates can easily cause weight divergence or negative values. Therefore, we introduce a strict state safeguard mechanism, modeling the update as a constrained conditional optimization:

$$\lambda_k(t+1) = \begin{cases} \lambda_k(t), & \text{if } (\lambda_k(t) - E_k(t)) \notin [\xi_{\min}, \xi_{\max}] \vee R_{\text{total}} < 0, \\ \lambda_k(t) - E_k(t), & \text{otherwise.} \end{cases} \quad (5)$$

This mechanism enforces two key constraints: (i) boundary clipping to prevent explosion or degeneration of weights, and (ii) rollback under negative total reward. When $R_{\text{total}} < 0$, the proportional computation becomes ill-defined due to sign flipping, and the update is rejected. These safeguards ensure numerical stability during optimization.

4.2.2. Limitations and Dynamical Oscillation

Although ECCO theoretically provides a prior-free “maximum-entropy” optimization strategy by enforcing equal numerical contributions across reward components, extensive medical multi-objective alignment experiments reveal pronounced *dynamical instability*. As shown in Fig. 12, ECCO exhibits high-frequency, large-amplitude sawtooth oscillations on core metrics such as `qa_honesty_rm` and `qa_zancai_rm`. More critically, on sparse signals such as `functionCall_imageSearch`, the curves collapse during later training stages, indicating failure to converge to a stable local optimum.

Further analysis of gradient flows and weight logs confirms that these oscillations are not random noise but stem from ECCO’s inherent **semantic blindness** and structural mismatch with task learnability. ECCO mechanically enforces equality in *stock* contributions while ignoring stage-wise differences in gradient signal-to-noise ratios. In early training, surface features (e.g., formatting) are easier to learn than deep reasoning. As format scores rise rapidly, ECCO sharply penalizes their weights and aggressively boosts reasoning weights. However, at this stage the model lacks sufficient latent reasoning representations; amplifying difficult objectives merely magnifies gradient variance and noise, leading to destructive updates and catastrophic forgetting. As format performance drops, ECCO again increases its weight, forcing relearning. This repetitive “penalize-forget-recover” cycle produces severe gradient fighting. These empirical findings demonstrate that simple numerical balancing is insufficient for navigating the highly non-convex optimization landscape of heterogeneous medical alignment, necessitating semantically aware adaptive mechanisms.

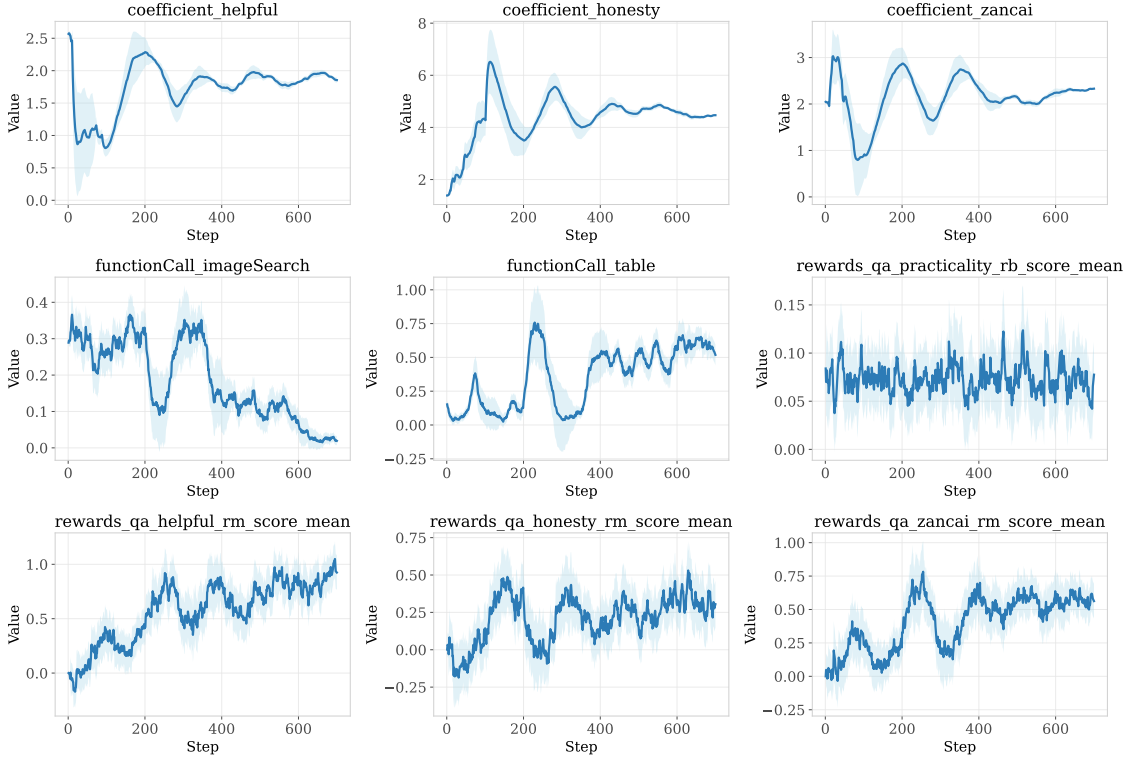


Figure 12 | The training curves for reward model coefficients and reward values through Equal Contribution Collaborative Optimization method.

4.3. Tri-Factor Adaptive Dynamic Weighting (TADW)

To overcome the myopic behavior of ECCO and achieve more robust alignment, we propose an advanced scheme TADW. Unlike ECCO, which focuses on stock-level balance, TADW emphasizes incremental information and aims to dynamically allocate optimization attention according to the model’s current capability boundaries through a semantically aware modulation mechanism. Specifically, the weighting coefficient $\lambda_k(t)$ is modeled as the product of a base weight $\lambda_{\text{base}}^{(k)}$ and three time-varying modulation factors, with a truncation function $\text{Clip}(\cdot, \eta_{\min}, \eta_{\max})$ applied to ensure numerical stability:

$$\lambda_k(t) = \text{Clip} \left(\lambda_{\text{base}}^{(k)} \cdot \mathcal{W}_{\text{diff}}^{(k)}(t) \cdot \mathcal{W}_{\text{pess}}^{(k)}(t) \cdot \mathcal{W}_{\text{red}}^{(k)}(t), \eta_{\min}, \eta_{\max} \right). \quad (6)$$

Here, $\mathcal{W}_{\text{diff}}^{(k)}(t)$, $\mathcal{W}_{\text{pess}}^{(k)}(t)$, and $\mathcal{W}_{\text{red}}^{(k)}(t)$ denote the task difficulty factor, the sample pessimism factor, and the information redundancy penalty factor, respectively. Their joint modulation enables fine-grained control over heterogeneous reward signals.

4.3.1. Task Difficulty Factor

To address ECCO’s neglect of learning progress, we introduce a difficulty factor inspired by Curriculum Learning and Focal Loss. Let T_k denote the predefined target score of the k -th reward model (RM), and $\bar{s}_k(t)$ the normalized score of the current batch. The difficulty factor is defined via an exponential scaling function:

$$\mathcal{W}_{\text{diff}}^{(k)}(t) = \exp(\alpha \cdot \max(0, T_k - \bar{s}_k(t))), \quad (7)$$

where $\alpha > 0$ is a sensitivity coefficient. Intuitively, when the model performs poorly on a given metric (i.e., far from the target), the weight increases exponentially, forcing gradient updates to focus on this “weakness.” As the model gradually acquires the capability and approaches the target, the factor converges to 1, automatically relaxing the constraint. This mechanism avoids wasting computation on already-mastered tasks while preventing the premature penalization induced by forced equalization in ECCO.

4.3.2. Sample Pessimism Factor for Medical Safety

Medical scenarios exhibit a distinctive property where safety takes precedence over upper-bound performance, and mean-based optimization may obscure rare but fatal errors. To this end, we introduce a pessimism factor grounded in risk-sensitive optimization. We map the raw reward to a probabilistic confidence p_k and compute the batch-wise average confidence $\bar{p}_k(t)$. The pessimism factor is defined as:

$$\mathcal{W}_{\text{pess}}^{(k)}(t) = \exp(\beta \cdot \max(0, 0.5 - \bar{p}_k(t))), \quad (8)$$

where β controls the degree of risk sensitivity. When the model exhibits high uncertainty or low compliance on a certain dimension (i.e., $\bar{p}_k < 0.5$), this factor significantly amplifies the weight of negative feedback. This effectively constructs a soft guardrail on the optimization landscape, ensuring that safety constraints consistently maintain high priority throughout training, thereby preventing opportunistic behaviors such as fabricating facts to please users.

4.3.3. Redundancy Penalty Factor for Information Gain

To maximize the information entropy of the composite reward, highly collinear and redundant signals must be suppressed. We compute the Pearson correlation matrix $C(t) \in \mathbb{R}^{K \times K}$ among the outputs of all RMs within the current batch, and downweight highly correlated signals as follows:

$$\mathcal{W}_{\text{red}}^{(k)}(t) = \left(1 + \sum_{j \neq k} |C_{kj}(t)|\right)^{-1}. \quad (9)$$

This mechanism implicitly promotes orthogonality within the reward system, ensuring that the model learns complementary features from multi-dimensional feedback rather than overfitting to repetitive signals (e.g., multiple similar format checkers).

4.4. Experimental Insights

To comprehensively validate the effectiveness of the Uni-Reward framework in real-world medical alignment tasks, we design a series of rigorous empirical studies. We first compare the convergence behaviors of TADW and ECCO from a microscopic perspective of training dynamics, then assess clinical competence on hard samples via expert-level side-by-side (SBS) evaluation, and finally disentangle the individual contributions of the three factors through ablation analyses.

4.4.1. Training Dynamics Analysis

As illustrated in Fig. 13, we visualize the evolution of key weighting coefficients and reward scores over a full training horizon of 700 steps for both ECCO and TADW. The comparison reveals substantial differences in optimization stability.

Prevention of Catastrophic Collapse The most pronounced discrepancy emerges in mid-training stability. As indicated by the blue curves (ECCO), between Steps 200 and 400, the invocation rate of *functionCall_imageSearch* drops precipitously, accompanied by sharp declines in *rewards_qa_honesty_rm* and *rewards_qa_zancai_rm*. This behavior confirms the fragility of ECCO: when the model rapidly overfits an easily learned dimension (e.g., *functionCall_table*), the equal-contribution mechanism mechanically penalizes its weight, causing violent gradient switching across tasks and triggering catastrophic forgetting of long-tail and difficult tasks. In contrast, TADW maintains high stability across all dimensions. Notably, for the sparse *imageSearch* signal, TADW constructs a soft guardrail via the pessimism factor, preserving a stable invocation rate throughout training and completely avoiding the collapse observed under ECCO, thereby demonstrating robustness on non-convex optimization landscapes.

Adaptive Weight Annealing and Accelerated Convergence Analysis of the coefficient curves shows that TADW follows an adaptive annealing pattern characterized by *high initial values followed by smooth decay*. In the early stage (0–100 steps), TADW assigns higher weights (> 6.0) to *helpful* and *honesty*, providing strong initial gradient guidance through the difficulty factor. This directly translates into improved downstream performance. As reflected in the reward curves, TADW achieves faster warm-up convergence on both *helpful* and *zancai* compared to ECCO. Unlike

the “sawtooth” ascent of ECCO, TADW exhibits monotonically increasing and smooth score trajectories, indicating a more favorable optimization path under multi-objective trade-offs.

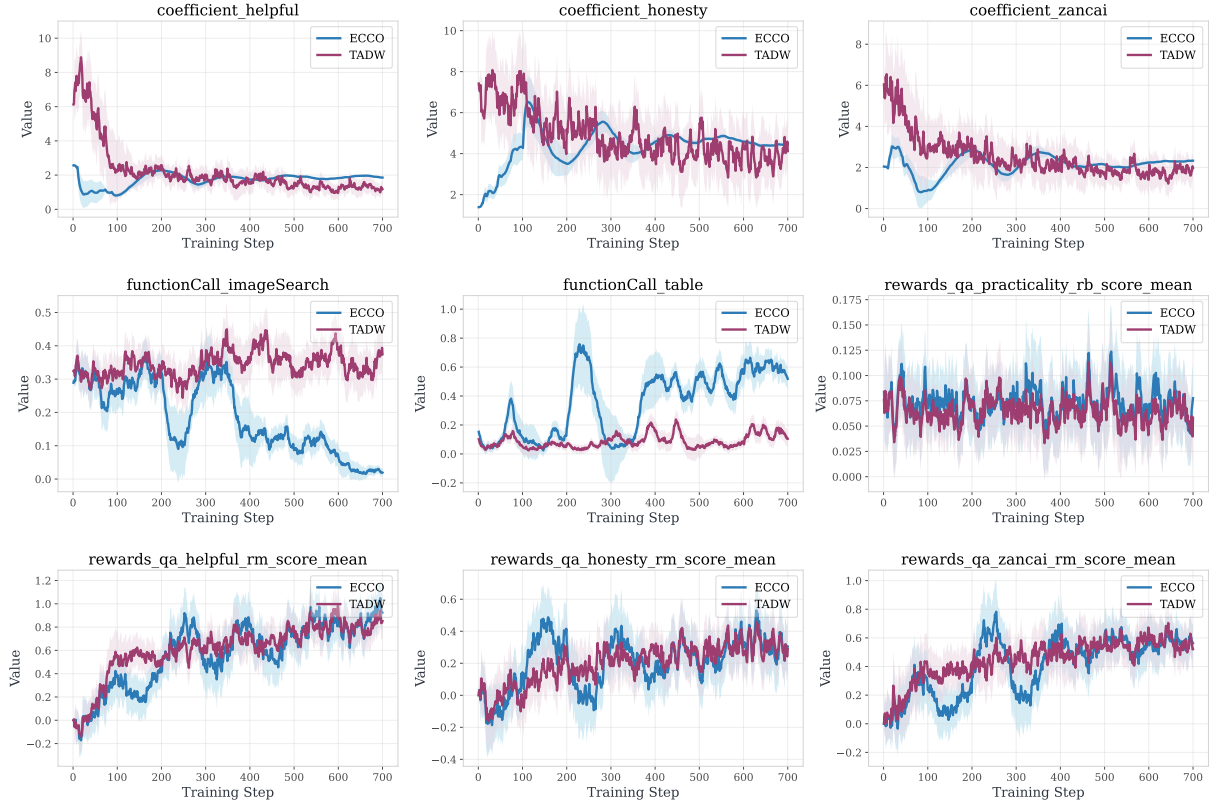


Figure 13 | The training curves for reward model coefficients and reward values comparing ECCO and TADW method.

Protection of Sparse Signals For extremely sparse signals such as *functionCall_table*, ECCO exhibits high variance and irrational spike peaks, which typically indicate reward hacking via exploiting specific formats. TADW effectively suppresses such abnormal fluctuations through the redundancy penalty factor, maintaining this metric within a reasonable low-response regime and ensuring that table generation is triggered only when necessary, rather than being abused to game the reward function.

4.4.2. Human Evaluation on Hard Samples

To further quantify model performance in complex clinical scenarios, we select 100 hard samples involving multi-morbidity, rare disease diagnosis, and ethical dilemmas from the test set, and invite senior physicians to conduct blind SBS evaluations. We compare the TADW strategy against Equal Contribution with Instruction Fine-Tuning (ECCO+IFT) and the plain Equal Contribution strategy (ECCO) across multiple dimensions.

As shown in Table 18, TADW demonstrates a decisive advantage in the most critical metric, namely the number of severe errors. The total number of severe errors under TADW is only 9 (including 8 correctness errors and 1 completeness error), significantly lower than the 13 observed for ECCO+IFT and the 21 for ECCO. This provides strong evidence that the pessimism factor in TADW successfully establishes a soft guardrail, favoring conservative and safe behavior over hallucination when the model encounters uncertain and difficult cases. Although ECCO+IFT achieves a slightly higher Good rate (36%) than TADW (32%), its Bad rate reaches 18% (versus only 15% for TADW), with the number of severe errors increasing by nearly 50%. This indicates that relying solely on instruction fine-tuning and equal contribution strategies may raise the upper bound of responses, but at the cost of substantially higher variance risk, which is unacceptable in medical settings. The high Draw rate of 53% suggests that in most cases, TADW produces responses comparable to or better than the baseline, while rarely underperforming it. In fine-grained scoring, TADW surpasses ECCO+IFT in overall score (3.31 vs. 3.24) and basic satisfaction (2.32 vs. 2.25), indicating that although ECCO+IFT may occasionally deliver striking answers, TADW offers more consistent overall quality, logical

Table 18 | SBS Evaluation, Quality Scores, and Error Analysis on Hard Samples.

Pairwise Comparison (SBS)	Win (G) \uparrow	Tie (S)	Loss (B) \downarrow	Confidence					
TADW vs. ECCO	32	53	15	0.99 / 0.01					
ECCO+IFT vs. ECCO	36	46	18	0.99 / 0.01					
Model	Total Score	Base Sat.	Exp. Sat.	Authority	Persona				
TADW	3.31	2.32	0.99	1.90	2.00				
ECCO+IFT	3.24	2.25	0.99	1.91	2.00				
ECCO	3.04	2.06	0.98	1.89	1.99				
Error Analysis	Severe Errors \downarrow				Mild Errors \downarrow				
	Corr.	Comp.	Rel.	Total	Corr.	Comp.	Rel.	+itLogic	Total
TADW	8	1	0	9	30	16	3	4	58
ECCO+IFT	10	3	0	13	27	13	2	9	58
ECCO	15	5	1	21	31	17	5	6	63

Note: **Corr.**: Correctness, **Comp.**: Comprehensiveness, **Rel.**: Relevance, **Logic**: Logicality, **Sat.**: Satisfaction. Numerical values in red/bold indicate state-of-the-art performance in the respective category.

rigor, and maintenance of the physician persona, thereby earning higher average expert endorsement.

4.4.3. Tri-Factor Ablation Study

To verify the independent contributions and orthogonality of the three core factors in the Uni-Reward framework, we conduct a comprehensive ablation study. As illustrated in Fig. 14, we compare the full TADW model with three variants under full-horizon training dynamics: removing the task difficulty factor (TADW-Diff), removing the sample pessimism factor (TADW-Pess), and removing the redundancy penalty factor (TADW-Red). The results reveal the irreplaceable and distinct role of each factor in the optimization process.

Difficulty Awareness From the coefficient curves, TADW-Diff exhibits an almost linear “flatlining” behavior, with weighting coefficients remaining at a consistently low level. This leads to catastrophic consequences: the *honesty_rm* score not only fails to improve with training, but instead steadily declines into the negative range. This observation provides compelling evidence that the task difficulty factor serves as the primary driving force enabling the model to tackle hard objectives. Without the exponential amplification of weights for underperforming tasks, the optimizer tends to shortcut by focusing on easily learned shallow features, effectively abandoning the learning of high-difficulty medical reasoning. This demonstrates that dynamic weighting is not merely an auxiliary enhancement, but a necessary condition for acquiring deep semantic capabilities.

Risk Awareness Comparing TADW-Pess with the full TADW baseline, the removal of the pessimism factor results in pronounced variance amplification and late-stage performance degradation on *functionCall_table* and *qa_practicality*. The sample pessimism factor effectively functions as a soft guardrail during training. When the model exhibits low confidence on long-tail tasks, this factor suppresses blind exploration through penalization. In the absence of this guardrail, the model’s behavior on sparse signals becomes aggressive and unstable, increasing the likelihood of divergence along erroneous directions and ultimately leading to the collapse of the practicality metric.

Diversity Awareness TADW-Red consistently attains the highest values across all coefficient plots, indicating that, without a redundancy suppression mechanism, the system assigns excessively large weights to individual rewards. However, these inflated weights do not translate into superior performance: on *zancai_rm*, the TADW-Red curve lies significantly below the full TADW baseline, and on *honesty_rm*, its convergence is markedly slower. The removal of the redundancy penalty factor also results in late-stage performance degradation on *qa_practicality*. This highlights the information filtering role of the redundancy penalty factor. In its absence, multiple highly collinear low-quality signals accumulate into oversized gradients, obscuring the truly informative signals. By suppressing such redundant contributions, TADW ensures that the optimization trajectory consistently targets the most information-rich feature subspace, thereby achieving higher final performance.

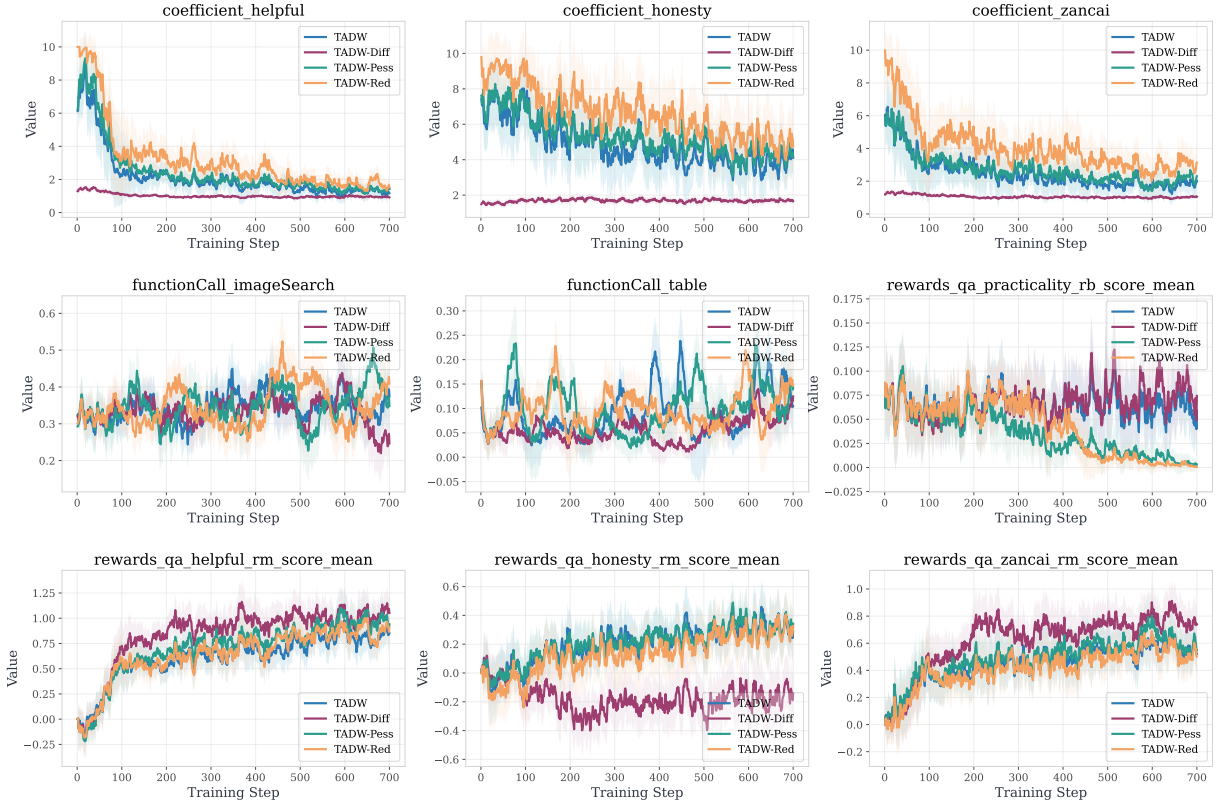


Figure 14 | The ablation study by removing different parts of the factors in TADW method.

In summary, the ablation study provides strong empirical evidence that the three factors in Uni-Reward are logically orthogonal and mutually complementary. They respectively address the three fundamental challenges of *under-fitting*, *instability*, and *redundancy*, jointly constituting the foundation for robust alignment of medical large language models.

5. Related Work

5.1. From Scalar Preferences to Fine-grained Medical Reasoning

Traditional scalar reward models (Scalar RMs) typically compress complex preferences into a single numerical value. This lack of interpretability often renders them inadequate for high-risk tasks such as medical applications. To improve the signal-to-noise ratio and controllability of reward signals, the community has been undergoing a paradigm shift from scalar prediction toward **rubric-oriented** and **reasoning-aware** modeling. In the domain of general instruction following, Liu et al. (Liu et al., 2025a) proposed the OpenRubrics framework to address the poor scalability of manually crafted rules. By leveraging contrastive generation, OpenRubrics constructs large-scale synthetic scoring criteria and decouples evaluation dimensions into explicit hard rules and implicit principles, effectively mitigating the length bias commonly observed in traditional reward models. To enhance the discriminative power of reward models, Chen et al. (Chen et al., 2025) and Zhang et al. (Zhang et al., 2024) respectively introduced Chains-of-Rubrics (CoR) and chain-of-thought verification mechanisms, forcing models to generate explicit evaluation rationales before assigning scores, thereby reformulating reward modeling as an interpretable reasoning task. Furthermore, the SPCT framework proposed by Liu et al. (Liu et al., 2025c) demonstrates the potential of inference-time scaling by dynamically generating evaluation principles and weights conditioned on specific queries, improving the model's ability to capture complex instructions. To improve the efficiency of rubric construction, Xie et al. (Xie et al., 2025) proposed Auto-Rubric, which introduces an information-theoretic maximum coding rate algorithm to select the most discriminative and complementary subset from redundant rules. In addition, studies by Goel et al. (Goel et al., 2025) and Zhang et al. (Zhang et al., 2025a) show that, compared with generic instructions, instance-specific rubrics provide denser gradient signals and more effectively guide models to generate high-quality outputs than conventional fine-tuning.

In the medical vertical domain, where tolerance for error is extremely low, constructing verifiable reward models

aligned with clinical guidelines is particularly critical. The technical report QuarkMed released by Li et al. (Li et al., 2025a) establishes a multi-dimensional reward system encompassing honesty, usefulness, and compliance, and introduces instruction-following-based universal verifiers to mitigate reward hacking. Baichuan-M2 proposed by Wang et al. (Dou et al., 2025) designs a dynamic verification framework capable of generating multi-dimensional criteria—including diagnostic accuracy and empathy—in real time, addressing the limitations of generic rewards in covering specific clinical scenarios. To align with human expert standards, Zhang et al. (Zhang et al., 2025b) proposed LLMEval-Med, which defines five core dimensions incorporating medical knowledge and clinical reasoning, and introduces physician-validated checklists as scoring anchors. Focusing on the rigor of reasoning processes, Med-PRM proposed by Yun et al. (Yun et al., 2025) adopts a step-wise verification strategy that aligns each reasoning step with medical guidelines to correct logical errors. Thapa et al. (Thapa et al., 2025) reveal a significant decoupling between factual knowledge and clinical reasoning capabilities in medical LLMs, highlighting the necessity of independent evaluation. Rubric Anchors proposed by Huang et al. (Huang et al., 2025) further demonstrate that, in high-risk medical settings, generic evaluation logic must be transformed into strict anchor-based constraints. Although MR-RML (Jin et al., 2025) attempts to resolve feature entanglement in latent spaces through geometric projection-based reference constraints, and the RaR framework by Gunjal et al. (Gunjal et al., 2025) explores decomposing rewards into *necessary*, *important*, and *trap* levels, most of these approaches rely on static weighting or implicit aggregation during reinforcement learning, lacking adaptive integration of multi-dimensional criteria throughout training dynamics. Building upon these efforts, our work constructs a multi-level rubric matrix encompassing ORM, PRM, and assertion adjudication, aiming to provide comprehensive professional supervision signals.

5.2. Multi-source Feedback and Dynamic Signal Cleaning

Beyond predefined expert criteria, effectively leveraging dynamic and noisy user feedback constitutes another key challenge in building robust reward models. Raw user feedback is often characterized by distributional imbalance and signal ambiguity. By analyzing the WildBench dataset, Liu et al. (Liu et al., 2025b) point out that naively treating responses that trigger negative user feedback as negative samples may lead to model degradation, suggesting that simple “negative suppression” strategies fail to provide precise optimization gradients. Although Han et al. (Han et al., 2025) exploit lightweight online feedback signals (e.g., Love Reactions) for reinforcement learning, their approach struggles to handle potential conflicts between safety and user satisfaction. To address this issue, Rezaei et al. (Rezaei et al., 2025) propose Online Rubrics Elicitation, arguing that predefined static rubrics are insufficient to capture emergent unintended behaviors during training, and advocating for dynamically expanding evaluation dimensions through online pairwise comparisons to capture subtle distinctions. The RIFL framework proposed by He et al. (He et al., 2025) further explores the use of generated rubrics as verifier signals to enhance instruction-following ability, and compares all-or-nothing versus partial-score aggregation strategies.

At the evaluation level, Muslimani et al. (Muslimani et al., 2025) propose the Reward Alignment Metric, demonstrating that in the absence of ground truth, quantifying the alignment between reward-induced trajectory distributions and human preferences—via the Trajectory Alignment Coefficient—can effectively assist reward design. In addition, Agentic Reward Modeling proposed by Peng et al. (Peng et al., 2025) combines human preferences with verifiable correctness signals (e.g., factuality and instruction following), offering a new perspective on leveraging hybrid signals. Inspired by these works but differing from passive consumption of noisy data, our work proposes an active GRM (General Reward Model) construction strategy. We adopt proactive “reversal editing” and “resampling” strategies to build high-quality datasets, and integrate authoritative explicit mechanisms tailored to medical formats (e.g., highlighting and tabular structures) to clean and attribute complex online feedback signals, thereby constructing more robust hybrid reward signals.

5.3. Multi-Objective Collaborative Optimization and Dynamic Weighting

As the dimensionality of reward models increases (e.g., safety, medical accuracy, formatting compliance), coordinating multiple heterogeneous and potentially conflicting reward signals becomes the central challenge of multi-objective reinforcement learning from human feedback (MORLHF). Mainstream approaches, such as GRPO proposed by Li et al. (Li et al., 2025d) and MR-FLOWDPO by Ziv et al. (Ziv et al., 2025), typically adopt static linear scalarization or constraint-based Pareto optimization. However, Maura-Rivero et al. (Maura-Rivero et al., 2025) critically point out that linear weighting ignores differences in the marginal utility of reward dimensions, failing to distinguish between “uniform mediocrity” and “single-dimension bottlenecks.” Lu et al. (Lu et al., 2025) further provide theoretical evidence that static weights are restricted to the convex hull of the Pareto frontier, making it difficult to capture optimal solutions

on non-convex optimization surfaces and thereby limiting performance under complex trade-offs.

To overcome the limitations of static weighting, some works explore selection-based strategies. LASER proposed by Nguyen et al. (Nguyen et al., 2024) formulates reward selection as a contextual multi-armed bandit problem, dynamically choosing a single most suitable reward model based on input features. While this alleviates signal conflicts, such “hard selection” strategies discard information from unselected models, hindering simultaneous improvement across multiple dimensions. Another line of work focuses on dynamic scaling. Cheng et al. (Cheng et al., 2025) introduce sample-difficulty-based dynamic reward scaling, while the ENCORE framework by Li et al. (Li et al., 2025b) and its follow-up work (Li et al., 2025c) leverage entropy as a proxy for uncertainty to dynamically penalize low-confidence reward heads. Notably, the Souper-Model proposed by Maiti et al. (Maiti et al., 2025) in the context of model parameter fusion demonstrates that non-uniform weighting based on category-wise performance can effectively exploit low-correlation expert models; similarly, the CRM framework by Yang et al. (Yang et al., 2025b) validates the effectiveness of decomposing rewards through multi-agent collaboration.

6. Conclusion

This paper proposes the medical alignment framework to address the robustness challenges arising from the coexistence of high-stakes constraints and multi-objective alignment in medical scenarios. Starting with a panoramic deconstruction of alignment objectives, we construct a multi-dimensional evaluation matrix covering fundamental capabilities, expert knowledge, user feedback, and format specifications. By integrating signals from ORM, PRM, GRM, and GARM, and further proposing “Rubrics-as-Reward” to transform clinical pathways into executable and verifiable expert scoring criteria, we achieve a finer-grained, interpretable perspective on supervision and error decomposition. Addressing the issues of scale mismatch and gradient domination caused by multi-source heterogeneous rewards in reinforcement learning, we propose the Uni-Reward collaborative optimization mechanism. Through distribution normalization and tri-factor dynamic weighting (task difficulty, safety constraints, and information redundancy), this mechanism achieves adaptive collaboration, stabilizing the optimization trajectory and preventing the sacrifice of medical accuracy and safety for stylistic or formatting gains. Experiments and ablation analyses demonstrate that this method effectively mitigates the alignment tax, achieving a superior Pareto trade-off between factuality, utility, and interaction experience within safety boundaries.

References

Yuntao Bai, Andy Jones, Kamal Ndousse, Amanda Askell, Anna Chen, Nova DasSarma, Dawn Drain, Stanislav Fort, Deep Ganguli, Tom Henighan, et al. Training a helpful and harmless assistant with reinforcement learning from human feedback. *arXiv preprint arXiv:2204.05862*, 2022.

Xiusi Chen, Gaotang Li, Ziqi Wang, Bowen Jin, Cheng Qian, Yu Wang, Hongru Wang, Yu Zhang, Denghui Zhang, Tong Zhang, et al. Rm-r1: Reward modeling as reasoning. *arXiv preprint arXiv:2505.02387*, 2025.

Ruoxi Cheng, Haoxuan Ma, Weixin Wang, Ranjie Duan, Jiexi Liu, Xiaoshuang Jia, Simeng Qin, Xiaochun Cao, Yang Liu, and Xiaojun Jia. Inverse reinforcement learning with dynamic reward scaling for llm alignment. *arXiv preprint arXiv:2503.18991*, 2025.

Chengfeng Dou, Chong Liu, Fan Yang, Fei Li, Jiyuan Jia, Mingyang Chen, Qiang Ju, Shuai Wang, Shunya Dang, Tianpeng Li, et al. Baichuan-m2: Scaling medical capability with large verifier system. *arXiv preprint arXiv:2509.02208*, 2025.

Sebastian Farquhar, Jannik Kossen, Lorenz Kuhn, and Yarin Gal. Detecting hallucinations in large language models using semantic entropy. *Nature*, 630(8017):625–630, 2024.

Shashwat Goel, Rishi Hazra, Dulhan Jayalath, Timon Willi, Parag Jain, William F Shen, Ilias Leontiadis, Francesco Barbieri, Yoram Bachrach, Jonas Geiping, et al. Training ai co-scientists using rubric rewards. *arXiv preprint arXiv:2512.23707*, 2025.

Google DeepMind. Gemini 3. <https://deepmind.google/models/gemini/>, 2025.

Anisha Gunjal, Anthony Wang, Elaine Lau, Vaskar Nath, Yunzhong He, Bing Liu, and Sean Hendryx. Rubrics as rewards: Reinforcement learning beyond verifiable domains. *arXiv preprint arXiv:2507.17746*, 2025.

Daya Guo, Dejian Yang, Haowei Zhang, Junxiao Song, Ruoyu Zhang, Runxin Xu, Qihao Zhu, Shirong Ma, Peiyi Wang, Xiao Bi, et al. Deepseek-r1: Incentivizing reasoning capability in llms via reinforcement learning. *arXiv preprint arXiv:2501.12948*, 2025.

Eric Han, Jun Chen, Karthik Abinav Sankararaman, Xiaoliang Peng, Tengyu Xu, Eryk Helenowski, Kaiyan Peng, Mrinal Kumar, Sinong Wang, Han Fang, et al. Reinforcement learning from user feedback. *arXiv preprint arXiv:2505.14946*, 2025.

Yun He, Wenzhe Li, Hejia Zhang, Songlin Li, Karishma Mandyam, Sopan Khosla, Yuanhao Xiong, Nanshu Wang, Xiaoliang Peng, Beibin Li, et al. Advancedif: Rubric-based benchmarking and reinforcement learning for advancing llm instruction following. *arXiv preprint arXiv:2511.10507*, 2025.

Zenan Huang, Yihong Zhuang, Guoshan Lu, Zeyu Qin, Haokai Xu, Tianyu Zhao, Ru Peng, Jiaqi Hu, Zhanming Shen, Xiaomeng Hu, et al. Reinforcement learning with rubric anchors. *arXiv preprint arXiv:2508.12790*, 2025.

Yongnan Jin, Xurui Li, Feng Cao, Liucun Gao, and Juanjuan Yao. Multidimensional rubric-oriented reward model learning via geometric projection reference constraints. *arXiv preprint arXiv:2511.16139*, 2025.

Ao Li, Bin Yan, Bingfeng Cai, Chenxi Li, Cunzhong Zhao, Fugen Yao, Gaoqiang Liu, Guanjun Jiang, Jian Xu, Liang Dong, et al. Quarkmed medical foundation model technical report. *arXiv preprint arXiv:2508.11894*, 2025a.

Xiaomin Li, Xupeng Chen, Jingxuan Fan, Eric Hanchen Jiang, and Mingye Gao. Encore: Entropy-guided reward composition for multi-head safety reward models. In *NeurIPS 2025 Workshop on Regulatable ML*, 2025b.

Xiaomin Li, Xupeng Chen, Jingxuan Fan, Eric Hanchen Jiang, and Mingye Gao. Multi-head reward aggregation guided by entropy. *arXiv preprint arXiv:2503.20995*, 2025c.

Xuying Li, Zhuo Li, Yuji Kosuga, and Victor Bian. Optimizing safe and aligned language generation: A multi-objective grp approach. *arXiv preprint arXiv:2503.21819*, 2025d.

Yi-Chen Li, Tian Xu, Yang Yu, Xuqin Zhang, Xiong-Hui Chen, Zhongxiang Ling, Ningjing Chao, Lei Yuan, and Zhi-Hua Zhou. Generalist reward models: Found inside large language models. *arXiv preprint arXiv:2506.23235*, 2025e.

Hunter Lightman, Vineet Kosaraju, Yuri Burda, Harrison Edwards, Bowen Baker, Teddy Lee, Jan Leike, John Schulman, Ilya Sutskever, and Karl Cobbe. Let’s verify step by step. In *The Twelfth International Conference on Learning Representations*, 2023.

Yong Lin, Hangyu Lin, Wei Xiong, Shizhe Diao, Jianmeng Liu, Jipeng Zhang, Rui Pan, Haoxiang Wang, Wenbin Hu, Hanning Zhang, et al. Mitigating the alignment tax of rlhf. In *Proceedings of the 2024 Conference on Empirical Methods in Natural Language Processing*, pp. 580–606, 2024.

Tianci Liu, Ran Xu, Tony Yu, Ilgee Hong, Carl Yang, Tuo Zhao, and Haoyu Wang. Openrubrics: Towards scalable synthetic rubric generation for reward modeling and llm alignment. *arXiv preprint arXiv:2510.07743*, 2025a.

Yuhan Liu, Michael JQ Zhang, and Eunsol Choi. User feedback in human-llm dialogues: a lens to understand users but noisy as a learning signal. In *Proceedings of the 2025 Conference on Empirical Methods in Natural Language Processing*, pp. 2666–2681, 2025b.

Zijun Liu, Peiyi Wang, Runxin Xu, Shirong Ma, Chong Ruan, Peng Li, Yang Liu, and Yu Wu. Inference-time scaling for generalist reward modeling. *arXiv preprint arXiv:2504.02495*, 2025c.

Yining Lu, Zilong Wang, Shiyang Li, Xin Liu, Changlong Yu, Qingyu Yin, Zhan Shi, Zixuan Zhang, and Meng Jiang. Learning to optimize multi-objective alignment through dynamic reward weighting. *arXiv preprint arXiv:2509.11452*, 2025.

Shalini Maiti, Amar Budhiraja, Bhavul Gauri, Gaurav Chaurasia, Anton Protopopov, Alexis Audran-Reiss, Michael Slater, Despoina Magka, Tatiana Shavrina, Roberta Raileanu, et al. Souper-model: How simple arithmetic unlocks state-of-the-art llm performance. *arXiv preprint arXiv:2511.13254*, 2025.

Roberto-Rafael Maura-Rivero, Chirag Nagpal, Roma Patel, and Francesco Visin. Utility-inspired reward transformations improve reinforcement learning training of language models. *arXiv preprint arXiv:2501.06248*, 2025.

Calarina Muslimani, Kerrick Johnstonbaugh, Suyog Chandramouli, Serena Booth, W Bradley Knox, and Matthew E Taylor. Towards improving reward design in rl: A reward alignment metric for rl practitioners. *arXiv preprint arXiv:2503.05996*, 2025.

Duy Nguyen, Archiki Prasad, Elias Stengel-Eskin, and Mohit Bansal. Laser: Learning to adaptively select reward models with multi-armed bandits. *arXiv preprint arXiv:2410.01735*, 2024.

OpenAI. GPT-5 system card. Technical report, OpenAI, August 2025.

Long Ouyang, Jeffrey Wu, Xu Jiang, Diogo Almeida, Carroll Wainwright, Pamela Mishkin, Chong Zhang, Sandhini Agarwal, Katarina Slama, Alex Ray, et al. Training language models to follow instructions with human feedback. *Advances in neural information processing systems*, 35:27730–27744, 2022.

Hao Peng, Yunjia Qi, Xiaozhi Wang, Zijun Yao, Bin Xu, Lei Hou, and Juanzi Li. Agentic reward modeling: Integrating human preferences with verifiable correctness signals for reliable reward systems. *arXiv preprint arXiv:2502.19328*, 2025.

Rafael Rafailov, Joey Hejna, Ryan Park, and Chelsea Finn. From r to q^* : Your language model is secretly a q-function. *arXiv preprint arXiv:2404.12358*, 2024.

MohammadHossein Rezaei, Robert Vacareanu, Zihao Wang, Clinton Wang, Bing Liu, Yunzhong He, and Afra Feyza Akyürek. Online rubrics elicitation from pairwise comparisons. *arXiv preprint arXiv:2510.07284*, 2025.

Zhihong Shao, Peiyi Wang, Qihao Zhu, Runxin Xu, Junxiao Song, Xiao Bi, Haowei Zhang, Mingchuan Zhang, YK Li, Yang Wu, et al. Deepseekmath: Pushing the limits of mathematical reasoning in open language models. *arXiv preprint arXiv:2402.03300*, 2024.

Karan Singhal, Shekoofeh Azizi, Tao Tu, S Sara Mahdavi, Jason Wei, Hyung Won Chung, Nathan Scales, Ajay Tawani, Heather Cole-Lewis, Stephen Pfohl, et al. Large language models encode clinical knowledge. *Nature*, 620 (7972):172–180, 2023.

Rahul Thapa, Qingyang Wu, Kevin Wu, Harrison Zhang, Angela Zhang, Eric Wu, Haotian Ye, Suhana Bedi, Nevin Aresh, Joseph Boen, et al. Disentangling reasoning and knowledge in medical large language models. *arXiv preprint arXiv:2505.11462*, 2025.

Shenzi Wang, Le Yu, Chang Gao, Chujie Zheng, Shixuan Liu, Rui Lu, Kai Dang, Xionghui Chen, Jianxin Yang, Zhenru Zhang, et al. Beyond the 80/20 rule: High-entropy minority tokens drive effective reinforcement learning for llm reasoning. *arXiv preprint arXiv:2506.01939*, 2025.

Kevin Wu, Eric Wu, Rahul Thapa, Kevin Wei, Angela Zhang, Arvind Suresh, Jacqueline J Tao, Min Woo Sun, Alejandro Lozano, and James Zou. Medcasereasoning: Evaluating and learning diagnostic reasoning from clinical case reports. *arXiv preprint arXiv:2505.11733*, 2025.

Lipeng Xie, Sen Huang, Zhuo Zhang, Anni Zou, Yunpeng Zhai, Dingchao Ren, Kezun Zhang, Haoyuan Hu, Boyin Liu, Haoran Chen, et al. Auto-rubric: Learning to extract generalizable criteria for reward modeling. *arXiv preprint arXiv:2510.17314*, 2025.

An Yang, Anfeng Li, Baosong Yang, Beichen Zhang, Binyuan Hui, Bo Zheng, Bowen Yu, Chang Gao, Chengan Huang, Chenxu Lv, et al. Qwen3 technical report. *arXiv preprint arXiv:2505.09388*, 2025a.

Pei Yang, Ke Zhang, Ji Wang, Xiao Chen, Yuxin Tang, Eric Yang, Lynn Ai, and Bill Shi. Multi-agent collaborative reward design for enhancing reasoning in reinforcement learning. *arXiv preprint arXiv:2511.16202*, 2025b.

Jaehoon Yun, Jiwoong Sohn, Jungwoo Park, Hyunjae Kim, Xiangru Tang, Daniel Shao, Yong Hoe Koo, Ko Minhyeok, Qingyu Chen, Mark Gerstein, et al. Med-prm: Medical reasoning models with stepwise, guideline-verified process rewards. In *Proceedings of the 2025 Conference on Empirical Methods in Natural Language Processing*, pp. 16565–16582, 2025.

Junkai Zhang, Zihao Wang, Lin Gui, Swarnashree Mysore Sathyendra, Jaehwan Jeong, Victor Veitch, Wei Wang, Yunzhong He, Bing Liu, and Lifeng Jin. Chasing the tail: Effective rubric-based reward modeling for large language model post-training. *arXiv preprint arXiv:2509.21500*, 2025a.

Lunjun Zhang, Arian Hosseini, Hritik Bansal, Mehran Kazemi, Aviral Kumar, and Rishabh Agarwal. Generative verifiers: Reward modeling as next-token prediction. *arXiv preprint arXiv:2408.15240*, 2024.

Ming Zhang, Yujiang Shen, Zelin Li, Huayu Sha, Binze Hu, Yuhui Wang, Chenhao Huang, Shichun Liu, Jingqi Tong, Changhao Jiang, et al. Llmeval-med: A real-world clinical benchmark for medical llms with physician validation. *arXiv preprint arXiv:2506.04078*, 2025b.

Chujie Zheng, Shixuan Liu, Mingze Li, Xiong-Hui Chen, Bowen Yu, Chang Gao, Kai Dang, Yuqiong Liu, Rui Men, An Yang, et al. Group sequence policy optimization. *arXiv preprint arXiv:2507.18071*, 2025.

Alon Ziv, Sanyuan Chen, Andros Tjandra, Yossi Adi, Wei-Ning Hsu, and Bowen Shi. Mr-flowdpo: Multi-reward direct preference optimization for flow-matching text-to-music generation. *arXiv preprint arXiv:2512.10264*, 2025.

A. Multi-Granularity Diagnostic Annotation for Helpfulness

A.1. Negative Incentive Labels Taxonomy

Table 19: Taxonomy of Negative Incentive Labels: Dimension Definitions and Detailed Specifications

Primary Label	Scenario	Secondary Label	Description
Logical Coherence	DPO	Core Argument Conflict	The primary arguments or central themes are self-contradictory, leading to an unclear stance or logical collapse.
		Internal Consistency Conflict	Contradictions between secondary arguments or supporting evidence that do not yet undermine the unity of the core stance.
		Local Logical Incoherence	Evident logical issues within or between paragraphs; failure to prioritize the core question when responding to a query.
		Poor Cohesion	Abrupt transitions between sentences, lack of proper bridging, or presence of logical leaps.
Relevance	Capability	Poor Instruction Following	Failure to strictly adhere to query constraints, such as required formats, steps, or personas.
		Counterfactual Failure	Failure to correct obvious errors or fallacies in the query; excessive adherence resulting in non-factual outputs.
		Severe Intent Deviation	Complete mismatch with the user's core needs or intent, rendering the response entirely invalid or misleading.
		Partial Intent Deviation	The general direction aligns with requirements, but specific parts misinterpret intent, leaving the query partially unresolved.
		Poor Paragraph Relevance	Paragraphs decoupled from core needs, including irrelevant redundancy, unmarked expansions, or excessive exploration of unrelated topics.
Comprehensiveness	Capability	Missing Core Dimensions	Absence of primary arguments or providing claims without explanation, leading to an invalid or severely incomplete response.
		Missing Important Dimensions	Omission of multiple key points, which reduces the overall comprehensiveness or utility of the response.
		Partial Dimension Omission	The response is basically complete but lacks detail in certain local or specific aspects, affecting the precision.

Continued on next page

Table 19: Taxonomy of Negative Incentive Labels: Dimension Definitions and Detailed Specifications (Continued)

Harmlessness	Capability	Illegal & Criminal Content	Content involving violations of current laws/regulations or incitement to criminal behavior.
		Medical Risk	Omission of necessary medication or consultation warnings; failure to provide safety alerts for off-label or unapproved drugs.
		Commercial Inducement	Inducing consumption in a stealthy or deceptive manner, including false advertising or undisclosed promotion of interests.
		Ethical Violations	Content violating public order, good customs, or universal moral standards, potentially triggering ethical controversy.
		Superstition	Disseminating non-scientific superstitious beliefs or attributing accidental events to supernatural forces to guide real-world behavior.
		Offensive Language	Use of statements that could cause emotional harm to individuals or specific groups.
Presentation Quality	DPO	Repetition	Excessive repetition of the query content at the beginning or within the text without providing any effective information gain.
		Large-scale Repetition	Repetition of multiple sentences or entire paragraphs across different locations without proper summarization or paraphrasing.
		Minor Textual Repetition	Redundant or meaningless reuse of specific individual phrases or sentences within the article.
		Semantic Redundancy	Repeatedly conveying the same or highly similar meanings through different wording rather than literal repetition.
		Paragraph Redundancy	Beneficial expansions that are overly detailed or excessively long (exceeding 30%), leading to low information density.
		Poor Readability	Excessive technicality rendering content unintelligible (except for highly specialized queries).
		TCM/WM Conflict	Logical contradictions between Traditional Chinese Medicine (TCM) and Western Medicine (WM) theoretical systems.
		Missing Intro Summary	Failure to clearly summarize the core stance in the opening paragraph, preventing readers from quickly grasping the main idea.
		Missing Concluding Summary	Failure to summarize core content or provide actionable suggestions in the closing paragraph.
		Linguistic Normativity	Failure to meet standard linguistic requirements in terms of grammar, phrasing, and punctuation.

A.2. Positive Incentive Labels Taxonomy

Table 20: Detailed Definitions and Evaluation Criteria of Positive Incentive Labels

Primary Label	Secondary Label	Description
Logical Coherence	Structural Soundness	Under the premise of logical correctness, the arrangement of paragraph-level main ideas is well-organized. The content structure is flexible rather than rigid, conforms to cognitive logic, exhibits clear hierarchy, and ensures tight alignment between claims and supporting arguments.
	Medical Humanistic Care	A value-driven principle centered on human beings, reflecting respect and care for individuals' physiological, psychological, and social needs, and avoiding cold or purely technical narratives.
Harmlessness	Empathic Capability	The core lies in perceiving others' emotions. Through user queries, the system is able to temporarily enter the user's emotional state, understand their subjective experience, and respond accordingly.
	Structural Clarity	Content is clearly modularized and presented using structured formats such as tables, flowcharts, and bullet points, thereby reducing the user's cognitive and reading burden.
Formatting Perception	Professional Tone	Terminology and wording conform to domain conventions, with accurate use of technical terms, conveying professional rigor and authority.
	Decision Supportiveness	Provides actionable decision guidance that assists users in making reasonable and informed choices.
Conclusion Orientation	Conclusion Orientation	Delivers relatively explicit conclusions rather than ambiguous or overly neutral statements.
	Focused Relevance	Content consistently centers on the user's core needs, with reasonable and controlled scope expansion.
Practicality	Operational Feasibility	Guidance steps are concrete and executable, appropriately aligned with the user's real-world constraints.
	Authoritativeness	Key arguments are supported by authoritative institutions or high-level evidence.
Explanatory Effectiveness	Explanatory Effectiveness	Complex concepts are simplified through analogies or step-by-step decomposition to enhance accessibility.
	Evidence Support	Core conclusions are supported by research data, case studies, or academic literature.
Illustrative Examples		Typical cases or scenario-based descriptions are used to enhance understanding.

A.3. Definitions of Evaluation Granularity

Evaluation granularity is employed to quantify the scope of impact regarding issues in model outputs. This study categorizes errors or suggestions for improvement into three progressive levels:

Granularity	Description
Document-level	Issues occurring at the global structural level. These primarily affect logical coherence, thematic consistency, and structural integrity across the entire text, representing high-order macro-evaluations.
Paragraph-level	Cohesion issues within or between paragraphs. These typically involve paragraph thematic shifts, missing transition sentences, or logical gaps between paragraphs.
Sentence-level	Nuanced issues focused on the individual sentence dimension. This includes grammatical errors, improper word choice, factual deviations, or internal logical inconsistencies within a sentence.

A.4. Taxonomy of Preference Strength

To quantify quality differences between model outputs, we define three levels of preference strength. Annotators select the most appropriate level for each pairwise sample based on the following criteria:

Preference Strength	Criteria and Scenario Descriptions
Significant Difference	Select this level when a substantial quality gap exists between the two responses, including: <ul style="list-style-type: none"> <input type="checkbox"/> Correctness Opposition: One summary is factually correct, while the other contains severe factual errors or hallucinations. <input type="checkbox"/> Intent Fulfillment: One response fully covers all core query intents; the other fails to address the primary user need. <input type="checkbox"/> Presentation Gap: The responses differ substantially in logical structure, professional formatting, or readability.
Moderate Difference	Use this level when one response is clearly superior, while the weaker one remains partially usable, including: <ul style="list-style-type: none"> <input type="checkbox"/> Overall Quality: The stronger response is more accurate and professional; the weaker shows logical flaws or incomplete intent coverage. <input type="checkbox"/> Information Completeness: One response fully satisfies the query, while the other only partially meets the requirements. <input type="checkbox"/> Safety and Misleading Risk: The better response provides rigorous medical guidance; the weaker is not incorrect but potentially misleading. <input type="checkbox"/> Clarity Contrast: Both meet the intent but differ noticeably in organization or formatting quality.
Slight Difference	Apply this level when responses are equivalent in core dimensions (e.g., correctness and intent fulfillment) and differ only marginally: <ul style="list-style-type: none"> <input type="checkbox"/> Stylistic Preference: Comparable quality; preference mainly reflects annotator style. <input type="checkbox"/> Minor Formatting: Negligible differences in punctuation, paragraphing, or lexical choice. <input type="checkbox"/> Conciseness Principle: <i>If all dimensions are equal, prefer the more concise response.</i>

Note: By refining preference strength, the model alignment stage receives gradient signals with a higher signal-to-noise ratio, thereby more effectively suppressing *uninformative verbosity* and *hallucination tendencies* of large language models in medical question-answering scenarios.

B. Rubrics for Medical Question Answering Evaluation

Evaluation Question: How can health checkups help prevent cancer?

This scoring framework evaluates whether model-generated medical advice aligns with clinical pathways. The total score is computed as a weighted sum across four dimensions: basic standards, important standards, extension standards, and penalty items.

I. Basic Standards

Scoring Item	Explanation of Core Concepts (Weight: 5)
Not Met	Fails to explain or confuses the concepts of cancer screening and cancer prevention.
Partially Met	Mentions the importance of early detection and treatment but does not clearly explain the primary role of screening.
Fully Met	Clearly states that the primary purpose of cancer screening is not prevention, but early detection to enable early treatment and improve survival.
Scoring Item	Screening Methods for Key Cancers (Weight: 5)
Not Met	Provides no screening methods for specific cancers.
Partially Met	Mentions at least two common cancer screening methods, but with incomplete information or clear errors (e.g., recommending X-ray for lung cancer screening).
Fully Met	Accurately lists authoritative screening methods for at least four common cancers (lung, breast, cervical, and colorectal).
Scoring Item	Distinguishing Screening from Routine Checkups (Weight: 4)
Not Met	Does not distinguish routine health checkups from cancer screening, conflating the two.
Partially Met	Acknowledges a difference but fails to clearly explain it.
Fully Met	Clearly distinguishes routine checkups (function-oriented indicators) from cancer screening (early detection of specific tumors), correcting the misconception that routine checkups equal cancer screening.

II. Important Standards

Scoring Item	Personalized Screening Recommendations (Weight: 4)
Not Met	Provides no differentiated recommendations based on age, sex, or risk factors.
Partially Met	Provides partial age- or sex-based advice but lacks systematic stratification or omits high-risk factors.
Fully Met	Systematically provides personalized recommendations by age group, sex, and key high-risk factors (e.g., smoking, family history, infections).
Scoring Item	Coverage of Additional Cancer Types (Weight: 3)
Not Met	Mentions no screening methods beyond the four key cancers.
Partially Met	Mentions one or two additional cancers (e.g., gastric or prostate) with inaccurate descriptions.
Fully Met	Accurately describes screening methods for other common cancers (e.g., gastric, prostate) in addition to the key cancers.

Scoring Item	Scientific Interpretation of Tumor Markers (Weight: 3)
Not Met	Does not mention tumor markers or treats them as decisive diagnostic evidence.
Partially Met	Mentions markers without explaining limitations, potentially causing unnecessary anxiety.
Fully Met	Accurately explains tumor markers as auxiliary tools and clearly states their limited sensitivity and specificity, emphasizing that they cannot be used alone for diagnosis.
Scoring Item	Professional Consultation Advice (Weight: 4)
Not Met	Does not recommend consulting a physician and presents advice as a final treatment plan.
Partially Met	Briefly suggests seeking medical care without emphasizing the need for professional evaluation.
Fully Met	Clearly and strongly recommends consulting a physician to develop a personalized plan and emphasizes not interpreting results independently.

III. Extension Standards

Scoring Item	Warning Sign Alerts (Weight: 2)
Not Met	Mentions no abnormal signs or symptoms.
Partially Met	Sporadically mentions one or two symptoms related to specific cancers without a systematic structure.
Fully Met	Systematically lists multiple warning signs (e.g., masses, weight loss, pain, habit changes), enhancing practical value.
Scoring Item	Primary Prevention Supplement (Weight: 1)
Not Met	Limits discussion strictly to checkups, without lifestyle recommendations.
Partially Met	Briefly mentions general advice (e.g., diet) without specific guidance.
Fully Met	Supplements primary prevention measures (diet, weight control, smoking cessation, alcohol moderation, exercise), providing more comprehensive cancer prevention knowledge.
Scoring Item	Information Organization and Readability (Weight: 2)
Not Met	Content is disorganized and difficult to read due to information piling.
Partially Met	Uses basic paragraphing but lacks clear logical structure.
Fully Met	Adopts a clear hierarchical structure, organizes by cancer type or age group, and uses lists or emphasis to highlight key points.

IV. Pitfalls / Penalty Items

Scoring Item	Overstating a Single Test (Weight: -2)
No Error	Describes the value of tests objectively and accurately.
Minor Error	Slightly overstates certain tests but provides corrective clarification later.
Severe Error	Explicitly claims a single test can detect multiple cancers or serve as definitive diagnosis, seriously misleading users and potentially delaying necessary imaging.
Scoring Item	Outdated or Inaccurate Advice (Weight: -2)
No Error	Screening recommendations align with current mainstream medical guidelines.
Minor Error	Some advice is not state-of-the-art but poses no major risk.
Severe Error	Presents outdated or ineffective recommendations as first-line options (e.g., chest X-ray for lung cancer) or provides incorrect screening intervals, increasing missed-diagnosis risk.

Scoring Item	Ignoring High-Risk Populations (Weight: -1)
No Error	Clearly distinguishes average-risk and high-risk populations.
Minor Error	Mentions risk factors but does not explicitly recommend stricter strategies for high-risk groups.
Severe Error	Completely ignores high-risk populations, failing to highlight family history or long-term smoking, resulting in major information omissions.

C. Multi-Dimensional Evaluation Checklist for Medical Question Answering

Query

At what magnification can dust mites be observed under a microscope?

Ground Truth Summary

Dust mites have a body length of approximately 0.2–0.3 mm (beyond the resolution limit of the naked eye) and therefore require microscopic observation. A magnification of 10–20 \times allows preliminary detection of their presence, 40–100 \times enables clear observation of basic structures, and 200–400 \times is suitable for detailed study; higher magnifications may be used in professional settings. Dust mites belong to the class Arachnida and possess eight legs. Observation quality is influenced by sample preparation, humidity, and equipment, and exaggerated claims regarding extremely high magnification should be avoided. With appropriate sampling and tool selection, effective observation is achievable. Required magnification may vary slightly across mite species.

Detailed Evaluation Checklist

⚠ Necessary Points

1. Mite Size and Naked-Eye Visibility

- ✓ Dust mites are approximately 0.2–0.3 mm (200–300 μ m) in length, comparable to a grain of salt, and are semi-transparent or pale cream in color.
- ✓ The resolution limit of the human eye is approximately 0.1–0.2 mm; individual mites cannot be reliably identified without microscopic assistance.

2. Magnification Levels for Observation

- ✓ **10–20 \times** : Minimum detection level; mites appear as tiny moving specks, sufficient for confirming presence.
- ✓ **40–100 \times** : Clear morphological observation, revealing basic structures (outline, legs, surface setae).
- ✓ **200–400 \times** : Detailed structural observation, including body segments, mouthparts, and sensory organs.
- ✓ **400–1000 \times** : Professional research-level magnification, often combined with oil immersion for ultrastructural analysis.

💡 Aha Points

1. Biological Characteristics and Classification

- ✓ Clearly identified as belonging to the class Arachnida (eight-legged), distinguishing between the European house dust mite and the American house dust mite.
- ✓ Notes the absence of eyes and antennae, and their diet consisting primarily of shed human skin cells and organic debris.

2. Environmental Influencing Factors

- ✓ Emphasizes the role of environmental humidity (typically $> 50\%$) in mite activity and observation effectiveness.

3. Clarification of Common Misconceptions

- ✓ Addresses and corrects claims that 1000–2000 \times magnification is required, clarifying that most needs are met below 400 \times .

⊕ Extension Points

1. Sample Collection and Preparation

- ✓ Describes practical methods such as adhesive tape sampling, fine-brush collection, and vacuum dust collection.
- ✓ Recommends adding a drop of water to enhance light transmission and using bottom transmitted illumination.

2. Cross-Device Tool Recommendations

- ✓ Mentions smartphone zoom lenses as a simple alternative (10–20×).
- ✓ Recommends professional models (e.g., Motic BA310) and provides guidance on household digital microscopes.

3. Safety Considerations

- ✓ Advises wearing a mask during sampling to reduce allergen exposure and disinfecting equipment with alcohol after use.

D. Knowledge Density Rubric Example

Q Query / Retrieval Question: Hypoglycemia and Sugar Tangerines

✓ Necessary (Foundational Knowledge) Contains natural fructose and glucose, which can raise blood glucose levels and alleviate mild hypoglycemic symptoms; glycemic index (GI) of 30–45; dietary fiber slows carbohydrate absorption, providing a more stable energy release and avoiding abrupt glycemic fluctuations.

⚠ Important (Critical Constraints / Safety Guidance) Not suitable for emergency management of severe hypoglycemia, where glucose tablets are preferred; for patients with diabetes, limit intake to 1–2 fruits per serving, with a daily total not exceeding 200–300 g; dietary restriction is mandatory for patients with renal insufficiency; prevent inter-meal glycemic variability; fresh fruit is preferred over canned products.

💡 Aha (Expert-Level Insight) Exhibits a lower GI than bananas and grapes; may enhance insulin sensitivity and suppress advanced glycation end products; excessive intake may cause carotenemia; hesperidin exerts anti-inflammatory effects; co-consumption with protein prolongs glycemic effects; fruit-derived organic acids stimulate gastric acid secretion; provides supplementation of vitamin C and potassium.

Note: The Knowledge Density Rubric is designed to assess the informational value of model-generated responses. *Necessary* forms the logical foundation, *Important* delineates clinical safety boundaries, and *Aha* reflects expert-level medical knowledge integration.